



# Modeling the effect of budget allocation on the abatement of atmospheric carbon dioxide

A. K. Misra<sup>1</sup> · Anjali Jha<sup>1</sup>

Received: 26 November 2021 / Revised: 18 April 2022 / Accepted: 8 May 2022 /

Published online: 9 June 2022

© The Author(s) under exclusive licence to Sociedade Brasileira de Matemática Aplicada e Computacional 2022

## Abstract

An increment in carbon dioxide (CO<sub>2</sub>) results in global warming posed a threat to the mankind. Mitigation of anthropogenic CO<sub>2</sub> emission is important for climate change alleviation. In this regard, some significant steps are taken by the government of every country, which requires budget. In this paper, to observe the effect of budget allocation on the abatement of atmospheric concentration of CO<sub>2</sub>, a non-linear mathematical model is formulated and analyzed. In the modeling process, it is considered that a part of the available budget is used for the control of anthropogenic emission and the remaining part of budget is used for afforestation and reforestation. For the proposed model, feasibility and stability of all the equilibria have been discussed. From the model analysis, we have derived that how much budget one should spend on controlling the anthropogenic emission of CO<sub>2</sub> and afforestation/reforestation. Furthermore, numerical simulation has been performed to support analytical findings. It has been shown that the atmospheric level of CO<sub>2</sub> can be reduced to an innocuous level if the efficacy of allocated budget to control the anthropogenic emission of CO<sub>2</sub> and afforestation/reforestation increases. Moreover, it is found that the growth rate of budget allocation due to an increase in atmospheric level of carbon dioxide may cause stability switch through Hopf-bifurcation.

**Keywords** Mathematical model · CO<sub>2</sub> gas · Forest biomass · Budget · Stability · Hopf-bifurcation

**Mathematics Subject Classification** 34D05 · 34D20 · 34D23

## 1 Introduction

Climate change is causing irreplaceable environmental damage. Sea-level rise, temperature rise, extreme weather conditions, and ocean acidification are some changes which have been

---

Communicated by Rafael Villanueva.

---

✉ Anjali Jha  
anjali\_jha1895@gmail.com

<sup>1</sup> Department of Mathematics, Institute of Science, Banaras Hindu University, Varanasi 221 005, India

pointed up in a recent report by UNCCS (UNCCS 2019). The increasing global temperature affects the freshwater availability, food security, and these in combination with extreme climatic events bring forth negative impacts on human health. IPCC 2018 has mentioned that the anthropogenic emission of greenhouse gases has warmed the atmosphere 1.0°C above the pre-industrial temperature level, and if the current emission rate of greenhouse gases persist, global temperature may increase to 1.5°C between the year 2030 and 2052 (IPCC 2018). As carbon dioxide (CO<sub>2</sub>) is a primary greenhouse gas due to its high presence in the atmosphere compared to other greenhouse gases, the enhanced concentration of this prime heat-trapping gas is predominantly accountable for global warming. The atmospheric level of CO<sub>2</sub> has elevated from 280 ppm (pre-industrial level) to 415 ppm in January 2021 (NOAA 2021). Recent emission gap report published by UNEP has reported that total carbon dioxide gas emission in 2018 amounted to 55.3 GtCO<sub>2</sub> of which 37.5 GtCO<sub>2</sub> is emitted due to fossil fuel burning and 3.5 GtCO<sub>2</sub> is emitted due to the land-use changes (UNEP 2019). This indicates that the anthropogenic emission of carbon dioxide is a root cause for such a high level of its atmospheric concentration. According to Shi (Shi 2003), 1.0% increment in the human population brings about 1.42% increment in carbon dioxide emission on average. Forest biomass also plays a prime role in the dynamics of atmospheric concentration of CO<sub>2</sub> as it acts as a carbon dioxide sink. Using mathematical models, it has been shown in articles that due to increasing human population, forest biomass is depleting rapidly (Cropper and Griffiths 1994; Misra *et al.* 2014; Shukla *et al.* 2011). In the FAO report (FAO 2020), it is stated that between 2010 and 2020, about 4.74 million hectares of forest had been cleared per year. This destruction in the natural sink of carbon dioxide is also a reason for such a high level of atmospheric concentration of CO<sub>2</sub> (Caetano *et al.* 2011). To stabilize the atmospheric level of CO<sub>2</sub> below 450 ppm, it is required to take some actions as soon as possible and continuously for few decades, and this could prevent some future severe adverse impacts (IPCC 2014).

To reduce the atmospheric concentration of carbon dioxide, it is required to make efforts. Some mitigation efforts use decarbonization technologies which control the anthropogenic emission of CO<sub>2</sub>, such as fuel switching, renewable energy, and carbon capture and storage (CCS). These techniques are discussed in the literature (Fawzy *et al.* 2020; Ricke *et al.* 2017; Wee 2013), and most of these techniques are well established and have low risk. Some mitigation techniques are termed as negative emission techniques, which include the techniques that capture CO<sub>2</sub> directly from the atmosphere, e.g., direct air capture and storage (DACS), ocean fertilization, afforestation/reforestation, etc., and these techniques are discussed in (Fawzy *et al.* 2020; IPCC 2018; Pires 2019; Smith *et al.* 2016). As combustion of fossil fuels occurs mainly in power sectors and industries, control of anthropogenic emission of CO<sub>2</sub> can be done here using the renewable energy, CCS technology as well as switching fuels to low carbon fuels. Vinca *et al.* have discussed about the decarbonization techniques, and they have mentioned that the leakage risk and high cost associated with the deployment of CCS technology are some points of concern of decarbonization techniques (Vinca *et al.* 2018). Maintaining the atmospheric level of CO<sub>2</sub> by controlling the anthropogenic emission using technological options has been studied in (Verma and Misra 2018). In this study, they have shown that using technological options, the atmospheric level of carbon dioxide can be controlled but high implementation cost of such options restrict their use at large scale. Other than that, the dismissive point of the negative emission technique such as afforestation and reforestation is that it requires a larger land which can increase the competition for the land between other land uses. According to Smith *et al.* (Smith *et al.* 2016), the removal of 1.1 GtCO<sub>2</sub> is possible by the year 2100 and this would require approximately 370 Mha new forest. Study of reduction in the atmospheric concentration of CO<sub>2</sub> using optimized afforestation has been done by Caetano *et al.* (Caetano *et al.* 2011). In some studies, it has been argued that

the negative emission techniques should be used together with decarbonization technologies to achieve a great mitigation effort (Gasser *et al.* 2015; Pires 2019). Moreover, utilizing finance on these technologies together with redirecting it to support land-use practices which are more sustainable, further to use it for the payments of sequestration of carbon can aid in the worth of forests to locals (FAO 2020) which can prevent deforestation. Moreover, a study done by Lata and Misra (Lata and Misra 2017) suggests that by providing the incentives to people, deforestation can be reduced. Some programs such as Unnat Jyoti, SLNP, National Electric Mobility Mission Plan, Pradhan Mantri Krishi Sinchayee Yojna, National Afforestation Program, National Green Highways Mission, etc. have been launched by the Indian government to maintain the atmospheric level of CO<sub>2</sub>. Till date, 30 projects of total expense INR 8,470 Million have been approved (MoEFCC 2021).

In recent years, effect of various factors like human population and related population pressure, forest biomass, environmental education, etc. on atmospheric concentration of CO<sub>2</sub> using mathematical models have been analyzed (Devi and Gupta 2020; Misra and Jha 2021; Misra and Verma 2013, 2015; Shukla *et al.* 2015; Tennakone 1990; Verma and Misra 2018). Tennakone has formulated a non-linear mathematical model by considering forestry biomass and atmospheric concentration of carbon dioxide as dynamic variables (Tennakone 1990). This study has shown that the excessive deforestation and rapid increase in atmospheric concentration of CO<sub>2</sub> destabilizes the system. Furthermore, Misra and Verma (Misra and Verma 2013) have presented a model to study the interplay between atmospheric concentration of CO<sub>2</sub>, human population, and forestry biomass. This study suggests that uncontrolled deforestation by the human population may lead the system to an unstable situation. Extending this study, Misra & Jha (Misra and Jha 2021) have shown that due to the increasing demand of human population for forestry biomass (i.e., population pressure), the atmospheric concentration of carbon dioxide increases. From these studies, it may be noted that controlling the anthropogenic emission of carbon dioxide or deforestation by the human population is important for stabilizing the atmospheric concentration of CO<sub>2</sub>. Devi and Gupta (Devi and Gupta 2020) have studied the effect of different types of biomass in controlling the atmospheric level of CO<sub>2</sub>. In the study done by Misra and Verma (Misra and Verma 2015), it has been shown that environmental education about the ill effects of increasing CO<sub>2</sub> to the population might be helpful in maintaining the atmospheric level of CO<sub>2</sub>.

From the above discussion, it may be noted that the atmospheric level of CO<sub>2</sub> can be maintained at an innocuous level using various decarbonization techniques or negative emission techniques, and for the implementation of these techniques government provide funds, (MoEFCC 2021). Therefore, it is reasonable to study the impact of allocated budget on the atmospheric level of carbon dioxide. In the present work, we formulate a non-linear mathematical model which explores the effect of budget allocation on the abatement of atmospheric concentration of carbon dioxide. For model formulation, we consider that the budget follows logistic growth and the allocated budget is used for two purposes; some proportion of the allocated budget is used for the application of various technologies or programs to reduce the anthropogenic emissions and remaining part of the budget is used to increase the forest by which sequestration of carbon dioxide increases.

## 2 Mathematical model

Let  $C(t)$ ,  $N(t)$ , and  $F(t)$  be the atmospheric level of CO<sub>2</sub>, human population, and forest biomass, respectively. The increasing level of atmospheric carbon dioxide is mainly respon-

sible for increasing global average temperature. Let  $C_0$  denotes the pre-industrial level of atmospheric  $CO_2$ . As the atmospheric level of carbon dioxide was almost constant during the pre-industrial period, we have taken  $C_0$  as a constant. The main cause behind the increased level of  $CO_2$  is its anthropogenic emission due to fossil fuel burning and land-use changes. In some studies, it has been discussed that the atmospheric level of  $CO_2$  can be maintained at an innocuous level using decarbonization techniques and negative emission techniques (Gasser *et al.* 2015; Pires 2019), and for the implementation of these techniques, the government provides funds. We have considered the allocated budget as a dynamical variable  $B(t)$ . Furthermore, we have considered that the budget allocated to maintain the atmospheric level of carbon dioxide follows the logistic growth. Moreover, the government provides additional funds if the atmospheric level of  $CO_2$  increases in excess amount; hence, the budget allocated by the government also depends upon the increased level of  $CO_2$  from its pre-industrial level  $C_0$ , so we have considered the term  $\eta(C - C_0)B$ . Here,  $\eta$  is per capita growth rate of budget in proportion to the increased level of carbon dioxide from its pre-industrial level. If there is already a high budget allocation for maintaining the atmospheric level of carbon dioxide, the budget will increase slowly. However, if the budget allocation is less, then on increase of atmospheric level of  $CO_2$ , the government will increase the budget rapidly. Thus, the dynamics of allocated budget  $B(t)$  is governed by the equation

$$\frac{dB}{dt} = rB \left( 1 - \frac{B}{K} \right) + \eta(C - C_0)B.$$

The anthropogenic emission of carbon dioxide depends upon the human population (Onozaki 2009), so we have considered that the anthropogenic emission rate of  $CO_2$  is proportional to the human population. The atmospheric concentration of  $CO_2$  depletes naturally and it is taken in proportion to the atmospheric concentration of  $CO_2$  (Nicol'skii 2010).  $\alpha$  is the natural depletion rate coefficient of atmospheric  $CO_2$ . The application of any mitigation strategies has some negative impacts too, such as CCS technique has cost disadvantage, leakage risk, etc. (Gibbins and Chalmers 2008). As, the technological options can be applied mainly in large industries, so it is not possible to achieve a net zero emission. Therefore, we have considered that the budget used for control of anthropogenic emission of  $CO_2$  has a limited impact on the control of anthropogenic emission of  $CO_2$ . Therefore, we have considered a saturated type of functional response to show the effect of budget on the control of anthropogenic emission of  $CO_2$ . We have considered that  $k^{th}$  ( $0 < k < 1$ ) part of the allocated budget is used for controlling the anthropogenic emission of  $CO_2$ . As the  $kB$  budget is used to control the anthropogenic emission of  $CO_2$ , therefore we have considered that the anthropogenic emission rate coefficient of  $CO_2$ , i.e.,  $\lambda$  decreases by a factor  $\frac{vkB}{q_1+kB}$ . Therefore, the net anthropogenic emission rate coefficient of  $CO_2$  becomes  $\left( \lambda - \frac{vkB}{q_1+kB} \right)$ , which is a decreasing function of the budget used to control the anthropogenic emission of  $CO_2$ . Here,  $v$  is the efficacy of budget allocated to control the anthropogenic emission of  $CO_2$  and  $q_1$  is a constant which is used to limit the effect of allocated budget in controlling the atmospheric level of  $CO_2$ . Also, the concentration of  $CO_2$  decreases due to its sequestration by forestry biomass during the photosynthesis process at a rate  $\lambda_1 CF$ . Therefore, the following differential equation governs the dynamics of atmospheric  $CO_2$  :

$$\frac{dC}{dt} = -\alpha(C - C_0) + \left( \lambda - \frac{vkB}{q_1+kB} \right) N - \lambda_1 CF.$$

Furthermore, the human population follows logistic growth with  $s$  and  $L$  as intrinsic growth rate and carrying capacity, respectively. Since the enhanced concentration of atmospheric

CO<sub>2</sub> has adverse effects on human health (Casper 2010), the population declines because of an increase in the atmospheric concentration of CO<sub>2</sub>. As human population clears forestry biomass for their livelihood (Cropper and Griffiths 1994; Shukla *et al.* 2011), we have considered that the growth rate of forest biomass decreases due to human population and this depletion of forestry biomass feedbacks to the growth of human population (Misra and Verma 2013; Shukla *et al.* 2011) with a proportionality constant  $\pi$ . Therefore, the dynamics of human population is governed by

$$\frac{dN}{dt} = sN \left( 1 - \frac{N}{L} \right) - \theta(C - C_0)N + \pi\phi NF.$$

Also, the forestry biomass follows logistic growth with  $u$  and  $M$  as intrinsic growth rate and carrying capacity of forestry biomass, respectively. The human population uses forest biomass for their livelihood, so the density of forest biomass decreases at a rate  $\phi NF$ . As mentioned above, forest biomass soaks carbon dioxide during the photosynthesis process. Hence, forest biomass acts as a natural sink of atmospheric carbon dioxide. Therefore, for maintaining the atmospheric level of carbon dioxide, increasing the forest biomass and controlling the anthropogenic emission of CO<sub>2</sub> might be beneficial. Therefore, we have considered that the remaining part of budget (i.e.,  $(1 - k)^{th}$  part) is used for the plantation of trees. Therefore, due to the allocated budget, the density of forest biomass increases at a rate  $\frac{\mu(1-k)BF}{q_2 + (1-k)B}$ ; here,  $\mu$  is efficacy of allocated budget for afforestation and reforestation programs and  $q_2$  is half-saturation constant which limits the effect of allocated budget. Here, again, we have considered the saturated type of functional response, because the available budget can increase the trees in the considered region up to a certain level. Therefore, the dynamics of forest biomass is governed by the following differential equation:

$$\frac{dF}{dt} = uF \left( 1 - \frac{F}{M} \right) - \phi NF + \left( \frac{\mu(1-k)B}{q_2 + (1-k)B} \right) F.$$

Thus, the set of non-linear differential equations governing the dynamics of atmospheric carbon dioxide according to our consideration is as follows:

$$\begin{aligned} \frac{dC}{dt} &= -\alpha(C - C_0) + \left( \lambda - \frac{\nu kB}{q_1 + kB} \right) N - \lambda_1 CF, \\ \frac{dN}{dt} &= sN \left( 1 - \frac{N}{L} \right) - \theta(C - C_0)N + \pi\phi NF, \\ \frac{dF}{dt} &= uF \left( 1 - \frac{F}{M} \right) - \phi NF + \left( \frac{\mu(1-k)B}{q_2 + (1-k)B} \right) F, \\ \frac{dB}{dt} &= rB \left( 1 - \frac{B}{K} \right) + \eta(C - C_0)B, \end{aligned} \tag{1}$$

where  $C(0) > C_0$ ,  $N(0) \geq 0$ ,  $F(0) \geq 0$  and  $B(0) \geq 0$ .

In general, the parameter  $q_1$  is the half-saturation constant, which represents the budget at which reduction in atmospheric level of CO<sub>2</sub> is half of its maximum possible reduction which can be achieved using budget. Similarly, we can define  $q_2$  for the forest biomass. The description of used parameters in model system (1) and their units are mentioned in Table 1.

**Lemma 1** *Region of attraction for the above model system is contained in  $\Omega$ :*

$$\Omega = \left\{ (C, N, F, B) \in \mathfrak{R}_+^4 : C_0 \leq C \leq C_m, 0 \leq N \leq N_m, 0 \leq F \leq F_m, 0 \leq B \leq B_m \right\}, \tag{2}$$

**Table 1** Parameters and their description with unit

Parameter	Description	Unit
$\alpha$	Natural depletion rate of CO <sub>2</sub>	(year) <sup>-1</sup>
$\lambda$	Aanthropogenic emission rate of carbon dioxide	ppm (person year) <sup>-1</sup>
$\lambda_1$	Absorption rate of CO <sub>2</sub> by forest biomass	(ton year) <sup>-1</sup>
$\nu$	Efficacy of budget to control the anthropogenic emission of CO <sub>2</sub>	ppm (person year) <sup>-1</sup>
$k$	Proportion of budget to control the anthropogenic emission of CO <sub>2</sub>	-
$q_1$	Half-saturation constant	dollar
$s$	Intrinsic growth of human population	(year) <sup>-1</sup>
$L$	Carrying capacity of human population	Person
$\theta$	Death rate of human population due to increased level of CO <sub>2</sub>	(ppm year) <sup>-1</sup>
$\pi$	Growth rate of human population due to forest biomass	Person (ton) <sup>-1</sup>
$\phi$	Deforestation rate	(person year) <sup>-1</sup>
$u$	Intrinsic growth of forest biomass	(year) <sup>-1</sup>
$M$	Carrying capacity of forest biomass	Ton
$\mu$	Efficacy of budget used for afforestation/reforestation	(year) <sup>-1</sup>
$q_2$	Half-saturation constant	Dollar
$C_0$	Pre-industrial level of CO <sub>2</sub>	ppm
$r$	Intrinsic growth rate of budget	(year) <sup>-1</sup>
$\eta$	Growth rate of budget	(ppm year) <sup>-1</sup>
$K$	Carrying capacity of budget	Dollar

where

$$C_m = C_0 + \frac{\lambda N_m}{\alpha}, N_m = \frac{L}{s} (s + \pi \phi F_m), F_m = \frac{M}{u} (u + \mu), B_m = \frac{K}{r} \left( r + \frac{\eta \lambda N_m}{\alpha} \right).$$

It attracts all the solutions initiating in the interior of positive orthant.

Proof of this lemma is given in Appendix A.

### Persistence

The permanence or persistence of the model system ensures that if the considered dynamical variables are initially present in the system, they will be present in the system for all future time. A system is said to be uniformly persistent if lower bound and upper bound of each positive solution exist, i.e., there exists positive constant  $M_1$  and  $M_2$ , such that each positive solution of the system with positive initial condition satisfies

$$M_1 \leq \liminf_{t \rightarrow \infty} W(t) \leq \limsup_{t \rightarrow \infty} W(t) \leq M_2,$$

where  $W(t) = (C(t), N(t), F(t), B(t))$ .

Proof of persistence of system (1) is given in Appendix B.

**Table 2** Obtained equilibria and condition for their existence

Equilibrium	Condition for existence
$E_0(C_0, 0, 0, 0)$	Without any condition
$E_1\left(C_0 + \frac{\lambda Ls}{(\alpha s + \theta \lambda L)}, \frac{\alpha s L}{(\alpha s + \theta \lambda L)}, 0, 0\right)$	Without any condition
$E_2\left(\frac{\alpha C_0}{\alpha + \lambda_1 M}, 0, M, 0\right)$	Without any condition
$E_3(C_0, 0, 0, K)$	Without any condition
$E_4(C_4, N_4, 0, B_4)$	$s - \theta(C_4 - C_0) > 0$
$E_5(C_5, N_5, F_5, 0)$	$u(s\alpha + \theta \lambda L) > \phi L \alpha s$
$E_6(C_6, 0, F_6, B_6)$	$\frac{\alpha r}{\eta} > M \lambda_1 \left(C_0 - \frac{r}{\eta}\right)$
$E^*(C^*, N^*, F^*, B^*)$	Stated in the existence part of $E^*$

### 3 Model analysis

As the formulated model (1) is non-linear, we perform its qualitative analysis using the stability theory of ordinary differential equations. To analyze the long-term behavior of the formulated model (1), first, we obtain the feasible equilibria and then perform their stability analysis.

#### 3.1 Equilibrium analysis

The equilibria are constant solutions of the model system (1). We can obtain them by setting the growth rate of dynamical variables to zero. All feasible equilibria for the model system (1) are listed in Table 2:

The existence of equilibria  $E_0, E_1, E_2$  and  $E_3$  are obvious, and hence omitted. Existence of  $E_4, E_5, E_6$  and  $E^*$  are shown below. In equilibrium  $E_4(C_4, N_4, 0, B_4)$ , the values of  $C_4, N_4$  and  $B_4$  are positive solutions of the following equations:

$$-\alpha(C - C_0) + \left(\lambda - \frac{vkB}{q_1 + kB}\right)N = 0, \tag{3}$$

$$s\left(1 - \frac{N}{L}\right) - \theta(C - C_0) = 0, \tag{4}$$

$$r\left(1 - \frac{B}{K}\right) + \eta(C - C_0) = 0. \tag{5}$$

From Eqs. (4) and (5), we have

$$N = \frac{L\{s - \theta(C - C_0)\}}{s} \text{ and } B = \frac{K\{r + \eta(C - C_0)\}}{r}.$$

Putting these values of  $N$  and  $B$  in Eq. (3), we have

$$-\alpha(C - C_0) + \left[\lambda - \frac{Kvk\{r + \eta(C - C_0)\}}{q_1 + \frac{Kk\{r + \eta(C - C_0)\}}{r}}\right] \left[\frac{L\{s - \theta(C - C_0)\}}{s}\right] = 0.$$

On simplifying this, we get

$$a(C - C_0)^2 - b(C - C_0) + c = 0,$$

where  $a = \left[ \frac{\alpha\eta kK}{r} + \frac{\lambda kKL\theta\eta}{rs} - \frac{vkKL\eta\theta}{rs} \right]$ ,  
 $b = -\alpha q_1 - \alpha kK - \frac{\lambda q_1 L\theta}{s} + \frac{\lambda kK\eta L}{r} - \frac{\lambda kKL\theta}{s} - \frac{vkKL\eta}{r} + \frac{vkKL\theta}{s}$ ,  
 $c = -[\lambda q_1 L + \lambda kKL - vkKL]$ .

As  $\lambda > v$ , implies  $a > 0$  and  $c < 0$  and the *discriminant*  $> 0$ . Thus, we have a positive real root (say  $\tilde{C}_4$ )  $\Rightarrow C = C_0 + \tilde{C}_4 = C_4$ .

Using this value of  $C_4$ , we get positive values of  $B_4$  and  $N_4$ , if  $[s - \theta(C_4 - C_0)] > 0$ , or we can say that the death rate of human population due to harmful effects of increased CO<sub>2</sub> should be lesser than its intrinsic growth rate.

In equilibrium  $E_5(C_5, N_5, F_5, 0)$ , the values of  $C_5, N_5$  and  $F_5$  are given as the solutions of the following equations:

$$-\alpha(C - C_0) + \lambda N - \lambda_1 CF = 0, \tag{6}$$

$$s \left( 1 - \frac{N}{L} \right) - \theta(C - C_0) + \pi\phi F = 0, \tag{7}$$

$$u \left( 1 - \frac{F}{M} \right) - \phi N = 0. \tag{8}$$

From Eq. (6), we have

$$C = \frac{\alpha C_0 + \lambda N}{\alpha + \lambda_1 F}. \tag{9}$$

Putting this value of  $C$  in Eq. (7), we get

$$N = \frac{L\{(s + \pi\phi F)(\alpha + \lambda_1 F) + \theta\lambda_1 C_0 F\}}{s(\alpha + \lambda_1 F) + \theta\lambda L}. \tag{10}$$

Using this value of  $N$  in equation (8), we get

$$\hat{a}F^2 + \hat{b}F + \hat{c} = 0.$$

$$\hat{a} = \left( \frac{su\lambda_1}{M} + \pi\phi^2 L\lambda_1 \right),$$

$$\hat{b} = -su\lambda_1 + \frac{u}{M}(s\alpha + \lambda\theta L) + \phi L(s\lambda_1 + \pi\phi\alpha + \theta\lambda_1 C_0),$$

$$\hat{c} = -(su\alpha + u\theta\lambda L - \phi L\alpha s).$$

As  $\hat{a} > 0$  and  $\hat{c} < 0$  provided  $su\alpha + u\theta\lambda L > \phi L\alpha s$ , also the *discriminant*  $> 0$ . Therefore, this quadratic equation gives a unique positive value of  $F$  provided that  $su\alpha + u\theta\lambda L > \phi L\alpha s$ . Using this value of  $F$  (say  $F_5$ ) in (10) and (9), we get the positive values of  $N$  and  $C$  (say  $N_5$  and  $C_5$ ), respectively.

In equilibrium  $E_6(C_6, 0, F_6, B_6)$ , the values of  $C_6, F_6$  and  $B_6$  are given by the solution of following equations:

$$-\alpha(C - C_0) - \lambda_1 CF = 0, \tag{11}$$

$$u \left( 1 - \frac{F}{M} \right) + \frac{\mu(1 - k)B}{q_2 + (1 - k)B} = 0, \tag{12}$$

$$r \left( 1 - \frac{B}{K} \right) + \eta(C - C_0) = 0. \tag{13}$$

From Eqs. (12) and (13), we get

$$F = \frac{M}{u} \left[ u + \frac{\mu(1 - k)B}{q_2 + (1 - k)B} \right] \text{ and } (C - C_0) = \frac{-r}{\eta} \left( 1 - \frac{B}{K} \right), \text{ respectively.}$$



Putting these values in equation (11), we get a quadratic equation in  $B$  as

$$\check{a}B^2 + \check{b}B + \check{c} = 0,$$

where  $\check{a} = \left[ \frac{\alpha r(1-k)}{\eta K} + \frac{M\lambda_1 r(u+\mu)(1-k)}{u\eta K} \right],$

$$\check{b} = \frac{-\alpha r(1-k)}{\eta K} + \frac{\alpha r q_2}{\eta K} + \frac{M\lambda_1(u+\mu)(1-k)}{u} \left( C_0 - \frac{r}{\eta} \right) + \frac{M\lambda_1 r q_2}{\eta K},$$

$$\check{c} = - \left[ \frac{\alpha r q_2}{\eta} - M\lambda_1 q_2 \left( C_0 - \frac{r}{\eta} \right) \right].$$

As,  $\check{a} > 0$  and  $\check{c} < 0$  provided that  $\frac{\alpha r}{\eta} > M\lambda_1 \left( C_0 - \frac{r}{\eta} \right)$  also the *discriminant*  $> 0$ . Therefore, we get a unique positive value of  $B$  (say  $B_6$ ). Using this value of  $B$ , positive value of  $C$  (from Eq. (11)) and  $F$  (from Eq. (12)) can be obtained.

The equilibrium  $E^*$  is given as the positive solution of the following equations:

$$-\alpha(C - C_0) + \left( \lambda - \frac{vkB}{q_1 + kB} \right) N - \lambda_1 CF = 0, \tag{14}$$

$$s \left( 1 - \frac{N}{L} \right) - \theta(C - C_0) + \pi\phi F = 0, \tag{15}$$

$$u \left( 1 - \frac{F}{M} \right) - \phi N + \frac{\mu(1-k)B}{q_2 + (1-k)B} = 0, \tag{16}$$

$$r \left( 1 - \frac{B}{K} \right) + \eta(C - C_0) = 0. \tag{17}$$

From Eqs. (17) and (15), we have

$$(C - C_0) = \frac{-r}{\eta} \left( 1 - \frac{B}{K} \right) \text{ and } N = \left[ \frac{L}{s} \left\{ s + \frac{r\theta}{\eta} \left( 1 - \frac{B}{K} \right) + \pi\phi F \right\} \right].$$

Using these values of  $C$  and  $N$  in Eqs. (14) and (16), we have

$$\begin{aligned} & \frac{\alpha r}{\eta} \left( 1 - \frac{B}{K} \right) + \left( \lambda - \frac{vkB}{q_1 + kB} \right) \left[ \frac{L}{s} \left\{ s + \frac{r\theta}{\eta} \left( 1 - \frac{B}{K} \right) + \pi\phi F \right\} \right] \\ & + \lambda_1 \left[ \frac{r}{\eta} \left( 1 - \frac{B}{K} \right) - C_0 \right] F = 0, \end{aligned} \tag{18}$$

$$u - \frac{uF}{M} - \frac{\phi L}{s} \left[ s + \frac{r\theta}{\eta} \left( 1 - \frac{B}{K} \right) + \pi\phi F \right] + \frac{\mu(1-k)B}{q_2 + (1-k)B} = 0. \tag{19}$$

From Eq. (18) when  $B = 0$ , we have  $F = \frac{\frac{r\alpha}{\eta} + \frac{\lambda L}{s} \left( s + \frac{r\theta}{\eta} \right)}{\lambda_1 \left[ C_0 - \frac{r}{\eta} \right] - \frac{\lambda L \pi \phi}{s}} > 0$  (say  $F_a$ ), provided that

$$\lambda_1 C_0 > \lambda_1 \frac{r}{\eta} + \frac{\lambda L \pi \phi}{s}.$$

When  $F = 0$ , we get a quadratic equation in  $B$  as

$$\begin{aligned} & \left[ -\frac{Lr\theta k(\lambda - v)}{s\eta K} - \frac{\alpha rk}{\eta K} \right] B^2 + \left[ \frac{\alpha rk}{\eta} - \frac{\alpha r q_1}{\eta K} - \frac{\lambda q_1 L r \theta}{s\eta K} + (\lambda - v) \frac{kL}{s} \left( s + \frac{r\theta}{\eta} \right) \right] B \\ & + \frac{\alpha r q_1}{\eta} + \frac{\lambda q_1 L}{s} \left( s + \frac{r\theta}{\eta} \right) = 0, \end{aligned}$$

which gives a positive root of  $B$ (say  $B_a$ ).

Differentiating equation (18) with respect to  $B$ , we have

$$\frac{dF}{dB} = \frac{\frac{\alpha r}{\eta K} + \frac{L}{s} \left\{ s + \frac{r\theta}{\eta} \left( 1 - \frac{B}{K} \right) + \pi \phi F \right\} \frac{vkq_1}{(q_1+kB)^2} + \left( \lambda - \frac{vkB}{q_1+kB} \right) \frac{Lr\theta}{\eta Ks} + \frac{r\lambda_1 F}{\eta K}}{\left( \lambda - \frac{vkB}{q_1+kB} \right) \frac{\pi \phi L}{s} + \frac{\lambda_1 r}{\eta} \left( 1 - \frac{B}{K} \right) - \lambda_1 C_0}$$

Therefore,  $\frac{dF}{dB} < 0$ .

From Eq. (19) when  $B = 0$ , we have

$$F = \frac{u - \frac{\phi L}{s} \left( s + \frac{r\theta}{\eta} \right)}{\frac{u}{M} + \frac{\pi \phi^2 L}{s}} > 0 \text{ (say } F_b),$$

provided  $u - \frac{\phi L}{s} \left( s + \frac{r\theta}{\eta} \right) > 0$ .

Putting  $F = 0$  in Eq. (19) and simplifying, we get

$$\begin{aligned} (1-k) \frac{r\theta}{\eta K} B^2 + \left[ (u + \mu)(1-k) + \frac{q_2 r \theta}{\eta K} - \frac{\phi L}{s} (1-k) \left( s + \frac{r\theta}{\eta} \right) \right] B \\ + \left[ uq_2 - \frac{q_2 \phi L}{s} \left( s + \frac{r\theta}{\eta} \right) \right] = 0. \end{aligned}$$

This gives negative root for  $B$ . Differentiating (19) with respect to  $B$ , we have

$$\frac{dF}{dB} = \frac{\frac{\phi L r \theta}{s \eta K} + \frac{\mu(1-k)q_2}{(q_2+(1-k)B)^2}}{\left( \frac{u}{M} + \frac{\pi \phi^2 L}{s} \right)} > 0.$$

Now, the isoclines (18) and (19) intersect at unique point  $(B^*, F^*)$  within the positive quadrant, provided that  $F_a > F_b$ , [see Fig. 1]. Therefore, there exists positive values for  $B$  and  $F$  provided that the following conditions hold:

- (i)  $\frac{\pi \phi \lambda L}{s} + \frac{\lambda_1 r}{\eta} < \lambda_1 C_0$ ,
- (ii)  $u - \frac{\phi L}{s} \left( s + \frac{r\theta}{\eta} \right) > 0$ ,
- (iii)  $\frac{u - \frac{\phi L}{s} \left( s + \frac{r\theta}{\eta} \right)}{\frac{u}{M} + \frac{\pi \phi^2 L}{s}} < \frac{\frac{\alpha r}{\eta} + \frac{\lambda L}{s} \left( s + \frac{r\theta}{\eta} \right)}{\lambda_1 C_0 - \frac{\pi \phi \lambda L}{s} - \frac{\lambda_1 r}{\eta}}$ .

Using this positive value of  $B^*$  and  $F^*$ , we get the positive value of  $C^*$  and  $N^*$ .

**Remark 1** Using the above equations, we can obtain that

$$\frac{dC^*}{dk} = \frac{\frac{r}{K} \left[ \frac{\lambda_1 s q_2 \mu C^* B^*}{L(q_2+(1-k)B^*)^2} - \frac{\pi \phi q_2 \mu B^* T}{(q_2+(1-k)B^*)^2} - \frac{q_1 v B^* P Q}{(q_1+kB^*)^2} \right]}{\frac{r}{K} \left[ \alpha P + \frac{\theta u T}{M} + \lambda_1 P R + \lambda_1 \theta \phi C^* \right] - \eta \left[ \frac{\pi \phi q_2 \mu (1-k) T}{(q_2+(1-k)B^*)^2} - \frac{q_1 v k P Q}{(q_1+kB^*)^2} - \frac{\lambda_1 s \pi \phi q_2 \mu (1-k) C^* B^*}{L(q_2+(1-k)B^*)^2} \right]}, \tag{20}$$

where  $P = \left( \frac{su}{LM} + \pi \phi^2 \right)$ ,  $Q = \left\{ \frac{su}{M} + \pi \phi u - \frac{\theta u}{M} (C - C_0) + \frac{\pi \phi \mu (1-k) B^*}{(q_2+(1-k)B^*)} \right\}$ ,  $R = \left\{ \left( \frac{su}{L} - \phi s \right) + \phi \theta (C - C_0) + \frac{\mu s (1-k) B^*}{L(q_2+(1-k)B^*)} \right\}$  and  $T = \left( \lambda - \frac{vkB^*}{q_1+kB^*} \right)$ .

From Eq. (20), we can say that when  $\frac{dC^*}{dk} < 0$ , the equilibrium level of concentration of atmospheric carbon dioxide decreases if the budget allocated to control the anthropogenic emission of carbon dioxide increases. Moreover, when  $\frac{dC^*}{dk} > 0$ , i.e.,  $\frac{dC^*}{d(1-k)} < 0$ , the equilibrium level of atmospheric concentration of carbon dioxide decreases with increase in proportion of allocated budget for afforestation/reforestation.

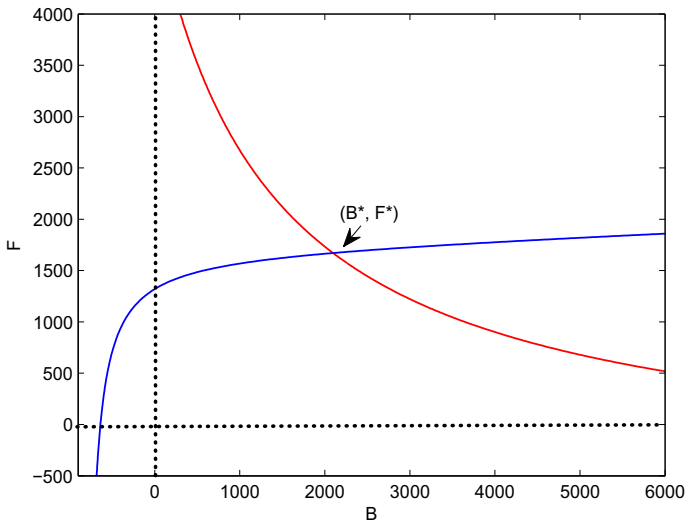


**Fig. 1** Isoclines (18) and (19) are plotted to validate the intersection at unique point  $(B^*, F^*)$  within interior of first quadrant

### 3.2 Local stability analysis of equilibria

Local stability of the equilibrium of the system is a property that a small change in the initial point of the formulated system has only a small effect in the behavior of solution as  $t \rightarrow \infty$ . In this part, we examine the stability of equilibria in a small neighborhood by analyzing the sign of eigenvalues of the Jacobian matrix corresponding to each equilibrium. The Jacobian matrix for the model system (1) is given by

$$J = \begin{bmatrix} -(\alpha + \lambda_1 F) \left( \lambda - \frac{vkB}{q_1 + kB} \right) - \lambda_1 C & \frac{-q_1 kvN}{(q_1 + kB)^2} \\ -\theta N & a_{22} & \pi \phi N & 0 \\ 0 & -\phi F & a_{33} & \frac{q_2 \mu (1-k) F}{(q_2 + (1-k)B)^2} \\ \eta B & 0 & 0 & r \left( 1 - \frac{2B}{K} \right) + \eta (C - C_0) \end{bmatrix},$$

where,  $a_{22} = s \left( 1 - \frac{2N}{L} \right) - \theta (C - C_0) + \pi \phi F$ ,  $a_{33} = u \left( 1 - \frac{2F}{M} \right) - \phi N + \frac{\mu (1-k) B}{q_2 + (1-k)B}$ .

Let the Jacobian matrix ( $J$ ) evaluated at equilibrium  $E_i$  ( $i = 0, 1, \dots, 6$ ) is represented by  $J_i$ .

Eigenvalues of  $J$  at  $E_0$  are  $-\alpha, s, u$  and  $r$ . Thus,  $E_0$  is locally unstable in  $N - F - B$  space and stable in  $C$ -direction.

Eigenvalues of  $J_1$  are  $u - \frac{\phi \alpha s L}{\alpha s + \lambda \theta L}$  and  $r + \frac{\eta \lambda L s}{\alpha s + \lambda \theta L}$  and remaining eigenvalues are either negative or have negative real part. As, the eigenvalue  $u - \frac{\phi \alpha s L}{\alpha s + \lambda \theta L}$  is positive whenever  $E_5$  exists. Therefore, the equilibrium  $E_1$  is stable in  $C - N$  plane, unstable in  $B$ -direction, and unstable in  $F$ -direction whenever  $E_5$  exists.

The eigenvalues of the Jacobian matrix  $J_2$  are  $-(\alpha + \lambda_1 M)$ ,  $s + \frac{\theta \lambda_1 C_0 M}{\alpha + \lambda_1 M} + \pi \phi M$ ,  $-u$  and  $r - \frac{\eta \lambda_1 C_0 M}{\alpha + \lambda_1 M}$ . From this, we can see that the eigenvalue  $r - \frac{\eta \lambda_1 C_0 M}{\alpha + \lambda_1 M}$  is positive whenever  $E_6$  exists. Thus, the equilibrium  $E_2$  is stable in  $C - F$  plane, unstable in  $N$ -direction, and unstable in  $B$ -direction whenever  $E_6$  exists.

Eigenvalues of  $J_3$  are  $-\alpha, s, u,$  and  $-r$ . Therefore,  $E_3$  is stable in  $C - B$  plane and unstable in  $N - F$  plane.

At equilibrium  $E_4$ , the Jacobian matrix has one eigenvalue  $u - \phi N_4 + \frac{\mu(1-k)B_4}{q_2+(1-k)B_4}$ , which is positive whenever  $E^*$  exists. Therefore,  $E_4$  is unstable in  $F$ -direction if  $E^*$  exists.

Furthermore, from the Jacobian matrix at  $E_5$ , we note that one eigenvalue is  $r + \eta(C_5 - C_0)$ , which is positive whenever  $E^*$  exists. Therefore,  $E_5$  is unstable in  $B$ -direction if  $E^*$  exists.

From the Jacobian matrix at  $E_6$ , we note that one eigenvalue is  $s - \theta(C_6 - C_0) + \pi\phi F_6$ , which is positive whenever  $E^*$  exists. Therefore,  $E_6$  is unstable in  $N$ -direction whenever  $E^*$  exists.

Moreover, to discuss the local stability of interior equilibrium  $E^*$ , we apply the Routh–Hurwitz criteria. The Jacobian matrix at  $E^*$  is given as follows:

$$J_{E^*} = \begin{bmatrix} -(\alpha + \lambda_1 F^*) \left( \lambda - \frac{vkB^*}{q_1+kB^*} \right) - \lambda_1 C^* & \frac{-q_1k v N^*}{(q_1+kB^*)^2} \\ -\theta N^* & -\frac{sN^*}{L} & \pi\phi N^* & 0 \\ 0 & -\phi F^* & -\frac{uF^*}{M} & \frac{q_2\mu(1-k)F^*}{(q_2+(1-k)B^*)^2} \\ \eta B^* & 0 & 0 & -\frac{rB^*}{K} \end{bmatrix}.$$

The characteristic polynomial of matrix  $J_{E^*}$  is given as

$$\rho^4 + A_1\rho^3 + A_2\rho^2 + A_3\rho + A_4 = 0, \tag{21}$$

where

$$\begin{aligned} A_1 &= \frac{uF^*}{M} + \frac{sN^*}{L} + \frac{rB^*}{K} + \check{\alpha}, \\ A_2 &= \eta B^* \check{c} + \phi^2 \pi F^* N^* + \frac{rB^*}{K} \frac{uF^*}{M} + \left( \frac{sN^*}{L} + \check{\alpha} \right) \left( \frac{rB^*}{K} + \frac{uF^*}{M} \right) + \frac{sN^*}{L} \check{\alpha} + \check{\theta} \theta N^*, \\ A_3 &= \lambda_1 \check{d} \eta C^* B^* + \left( \frac{sN^*}{L} + \frac{uF^*}{M} \right) \eta B^* \check{c} + \phi^2 \pi N^* F^* \left( \frac{rB^*}{K} + \check{\alpha} \right) + \lambda_1 \theta \phi N^* C^* F^* \\ &\quad + \left( \frac{sN^*}{L} + \check{\alpha} \right) \frac{rB^*}{K} \frac{uF^*}{M} + \left( \frac{rB^*}{K} + \frac{uF^*}{M} \right) \frac{sN^*}{L} \check{\alpha} + \left( \frac{rB^*}{K} + \frac{uF^*}{M} \right) \check{\theta} \theta N^*, \\ A_4 &= \eta \lambda_1 \check{d} \frac{sN^*}{L} C^* B^* + \eta \check{c} B^* \frac{sN^*}{L} \frac{uF^*}{M} - \eta \pi \phi \check{b} \check{d} B^* N^* + \pi \phi^2 \eta \check{c} B^* N^* F^* \\ &\quad + \phi^2 \pi \check{\alpha} \frac{rB^*}{K} F^* N^* + \lambda_1 \theta \phi \frac{rB^*}{K} N^* C^* F^* + \frac{rB^*}{K} \frac{uF^*}{M} \frac{sN^*}{L} \check{\alpha} + \frac{rB^*}{K} \frac{uF^*}{M} \check{\theta} \theta N^*. \end{aligned}$$

Here,  $\check{\alpha} = (\alpha + \lambda_1 F^*), \check{b} = \left( \lambda - \frac{vkB^*}{q_1+kB^*} \right), \check{c} = \frac{q_1k v N^*}{(q_1+kB^*)^2}, \check{d} = \frac{q_2\mu(1-k)F^*}{(q_2+(1-k)B^*)^2}$ .

From above, we can note that  $A_i > 0$  for  $i = 1, 2, 3, 4$ . Applying Routh–Hurwitz criteria, it can be deduced that all the roots of Eq. (21) are either negative or have negative real part iff

$$A_3(A_1A_2 - A_3) - A_1^2A_4 > 0. \tag{22}$$

The local stability of  $E^*$  depicts that if any initial start is taken inside some small neighborhood of  $E^*(C^*, N^*, F^*, B^*)$ , the solution trajectories will always approach to  $E^*(C^*, N^*, F^*, B^*)$  as  $t \rightarrow \infty$ , i.e., the system will eventually get stabilized.

### 3.3 Non-linear stability analysis

In this section, the region for stability analysis of the interior equilibrium  $E^*$  is extended from a small neighborhood to the whole region of attraction. To investigate the non-linear stability of the interior equilibrium, we use Liapunov’s method.

Consider a positive definite function ‘ $V$ ’ as

$$V = \frac{1}{2}(C - C^*)^2 + m_1 \left( N - N^* - N^* \ln \frac{N}{N^*} \right) + m_2 \left( F - F^* - F^* \ln \frac{F}{F^*} \right) + m_3 \left( B - B^* - B^* \ln \frac{B}{B^*} \right).$$

On differentiating ‘ $V$ ’ with respect to ‘ $t$ ’ along the solution of system (1), we have

$$\begin{aligned} \frac{dV}{dt} = & -(\alpha + \lambda_1 F^*)(C - C^*)^2 - \frac{m_1 s}{L}(N - N^*)^2 - \frac{m_2 u}{M}(F - F^*)^2 - \frac{m_3 r}{K}(B - B^*)^2 \\ & + \left( \lambda - m_1 \theta - \frac{vkB^*}{q_1 + kB^*} \right) (N - N^*)(C - C^*) \\ & + (m_1 \pi \phi - m_2 \phi)(F - F^*)(N - N^*) \\ & - \lambda_1 C(C - C^*)(F - F^*) - \frac{vkq_1 N}{(q_1 + kB)(q_1 + kB^*)}(C - C^*)(B - B^*) \\ & + m_3 \eta(C - C^*)(B - B^*) + \frac{m_2 \mu(1 - k)q_2}{(q_2 + (1 - k)B)(q_2 + (1 - k)B^*)}(F - F^*)(B - B^*). \end{aligned}$$

Choosing  $m_1 = \frac{1}{\theta} \left( \lambda - \frac{vkB^*}{q_1 + kB^*} \right)$  and  $m_2 = m_1 \pi = \frac{\pi}{\theta} \left( \lambda - \frac{vkB^*}{q_1 + kB^*} \right)$ , we have

$$\begin{aligned} \frac{dV}{dt} = & -(\alpha + \lambda_1 F^*)(C - C^*)^2 - \frac{s}{\theta L} \left( \lambda - \frac{vkB^*}{q_1 + kB^*} \right) (N - N^*)^2 - \frac{m_3 r}{K}(B - B^*)^2 \\ & - \frac{u\pi}{\theta M} \left( \lambda - \frac{vkB^*}{q_1 + kB^*} \right) (F - F^*)^2 - \lambda_1 C(C - C^*)(F - F^*) \\ & - \frac{vkq_1 N}{(q_1 + kB)(q_1 + kB^*)}(B - B^*)(C - C^*) + m_3 \eta(C - C^*)(B - B^*) \\ & + \frac{\pi}{\theta} \left( \lambda - \frac{vkB^*}{q_1 + kB^*} \right) \frac{\mu(1 - k)q_2}{(q_2 + (1 - k)B)(q_2 + (1 - k)B^*)}(F - F^*)(B - B^*). \end{aligned}$$

Therefore,  $\frac{dV}{dt}$  is negative definite if the following conditions hold:

$$\lambda_1^2 C_m^2 < \frac{2\pi u}{3\theta M} (\alpha + \lambda_1 F^*) \left( \lambda - \frac{vkB^*}{q_1 + kB^*} \right), \tag{23}$$

$$\frac{\mu^2(1 - k)^2 \pi}{(q_2 + (1 - k)B^*)^2 \theta} \left( \lambda - \frac{vkB^*}{q_1 + kB^*} \right) < \frac{2ru}{3KM} m_3, \tag{24}$$

$$\frac{v^2 k^2 N_m^2}{(q_1 + kB^*)^2} < \frac{4m_3 r}{9K} (\alpha + \lambda_1 F^*), \tag{25}$$

$$m_3 \eta^2 < \frac{4r}{9K} (\alpha + \lambda_1 F^*). \tag{26}$$

Using inequalities (24), (25), and (26), value of constant  $m_3 > 0$  can be chosen, provided that the following given condition holds:

$$\max\{S_1, S_2\} < \frac{4r^2}{9\eta^2 K^2}(\alpha + \lambda_1 F^*),$$

where  $S_1 = \frac{3M\pi}{2u\theta} \left( \lambda - \frac{vkB^*}{q_1+kB^*} \right) \frac{\mu^2(1-k)^2}{(q_2+(1-k)B^*)^2}$ ,  $S_2 = \frac{9v^2k^2N_m^2}{4(q_1+kB^*)^2(\alpha+\lambda_1F^*)}$ .

Therefore, we can state the following theorem for the non-linear stability of interior equilibrium  $E^*$ .

**Theorem 1** *The interior equilibrium  $E^*$ , if exists, is non-linearly stable inside  $\Omega$  if the following inequalities hold:*

$$\lambda_1^2 C_m^2 < \frac{2\pi u}{3\theta M}(\alpha + \lambda_1 F^*) \left( \lambda - \frac{vkB^*}{q_1+kB^*} \right)$$

$$\max\{S_1, S_2\} < \frac{4r^2}{9\eta^2 K^2}(\alpha + \lambda_1 F^*),$$

where  $S_1$  and  $S_2$  are given above.

**Remark 2** The ecological interpretation of above conditions stated in Theorem 1 is that if these conditions are fulfilled, the interior equilibrium  $E^*$  will be globally stable, i.e., for any initial condition inside the region of attraction, the solution trajectories will always approach to the interior equilibrium. From the obtained condition, we can interpret that for large values of  $\lambda_1$  and  $\eta$ , the conditions may be violated and the formulated model system (1) may become unstable. Therefore, we can say that  $\lambda_1$  and  $\eta$  have destabilizing effect on the system’s dynamics. However, for large values of  $r$ , the obtained conditions are easily satisfied, so the parameter  $r$  has a stabilizing effect on the system’s dynamics.

### 4 Existence of Hopf-bifurcation

We have noticed that the obtained condition for the local stability of interior equilibrium given in Eq. (22) is satisfied for small values of parameter  $\eta$ . However, on increasing the value of  $\eta$ , the local stability condition may be violated. Hence, there is a possibility of existence of Hopf-bifurcation around the interior equilibrium  $E^*$  with respect to parameter  $\eta$ . In this part, conditions for existence of Hopf-bifurcation around the interior equilibrium  $E^*$  by taking  $\eta$  as a bifurcation parameter have been derived. The characteristic equation of the Jacobian matrix around  $E^*$  is given by (21) and every term of the characteristic polynomial can be expressed in terms of  $\eta$ , so we can write it as

$$\rho^4 + A_1(\eta)\rho^3 + A_2(\eta)\rho^2 + A_3(\eta)\rho + A_4(\eta) = 0. \tag{27}$$

At the critical value of  $\eta = \eta_c$

$$A_3(\eta_c)(A_1(\eta_c)A_2(\eta_c) - A_3(\eta_c)) - A_1^2(\eta_c)A_4(\eta_c) = 0. \tag{28}$$

Therefore, at  $\eta_c$ , we get the reduced characteristic equation as

$$\left( \rho^2 + \frac{A_3}{A_1} \right) \left( \rho^2 + A_1\rho + \frac{A_1A_4}{A_3} \right) = 0. \tag{29}$$

The above equation has four roots say  $\rho_j$  ( $j = 1, 2, 3, 4$ ) with a pair of purely imaginary roots  $\rho_{1,2} = \pm i\omega_0$ , where  $\omega_0 = \left(\frac{A_3}{A_1}\right)^{\frac{1}{2}}$ . The nature of other two roots  $\rho_3$  and  $\rho_4$  can be identified as

$$\rho_3 + \rho_4 = -A_1, \tag{30}$$

$$\omega_0^2 + \rho_3\rho_4 = A_2, \tag{31}$$

$$\omega_0^2(\rho_3 + \rho_4) = -A_3, \tag{32}$$

$$\omega_0^2\rho_3\rho_4 = A_4. \tag{33}$$

From (30) and (33), if  $\rho_3$  and  $\rho_4$  are real, then they are negative. If the roots are complex, from (30), we have  $2\text{Re}(\rho_3) = -A_1$ , i.e.,  $\rho_3$  and  $\rho_4$  are complex eigenvalues with negative real parts. By this, we can conclude that other two roots ( $\rho_3$  and  $\rho_4$ ) have negative real part. This ensures the occurrence of Hopf-bifurcation.

Moreover, let  $\eta \in (\eta_c - \epsilon, \eta_c + \epsilon)$ , then the two eigenvalues will be  $\rho_{1,2} = \sigma \pm i\varepsilon$ . Using this value in Eq. (27) and separating the real and imaginary parts, respectively, we have

$$\sigma^4 + A_1\sigma^3 + A_2\sigma^2 + A_3\sigma + A_4 + \varepsilon^4 - 6\sigma^2\varepsilon^2 - 3A_1\sigma\varepsilon^2 - A_2\varepsilon^2 = 0, \tag{34}$$

$$4\sigma\varepsilon(\sigma^2 - \varepsilon^2) - A_1\varepsilon^3 + 3A_1\sigma^2\varepsilon + 2A_2\sigma\varepsilon + A_3\varepsilon = 0. \tag{35}$$

As  $\varepsilon(\eta) \neq 0$ , from Eq. (35) we have

$$-(4\sigma + A_1)\varepsilon^2 + 4\sigma^3 + 3A_1\sigma^2 + 2A_2\sigma + A_3 = 0.$$

Putting this value of  $\varepsilon^2$  in Eq. (34) and then differentiating this with respect to  $\eta$  and substituting  $\varepsilon(\eta_c) = 0$  in it, we have

$$\left[\frac{d\sigma}{d\eta}\right]_{[\eta=\eta_c]} = \left[\frac{\frac{d}{d\eta}(A_1A_2A_3 - A_3^2 - A_1^2A_4)}{-2A_1(A_1A_3 + (2\frac{A_3}{A_1} - A_2)^2)}\right]_{[\eta=\eta_c]}. \tag{36}$$

Thus,  $\left[\frac{d\sigma}{d\eta}\right]_{[\eta=\eta_c]} \neq 0$

$$\text{if } \left[\frac{\frac{d}{d\eta}(A_1A_2A_3 - A_3^2 - A_1^2A_4)}{-2A_1(A_1A_3 + (2\frac{A_3}{A_1} - A_2)^2)}\right]_{[\eta=\eta_c]} \neq 0. \tag{37}$$

Therefore, the transversality condition is

$$\left[\frac{\frac{d}{d\eta}(A_1A_2A_3 - A_3^2 - A_1^2A_4)}{-2A_1(A_1A_3 + (2\frac{A_3}{A_1} - A_2)^2)}\right]_{[\eta=\eta_c]} \neq 0.$$

Hence, we have the following theorem;

**Theorem 2** *At  $\eta = \eta_c$ , the system (1) undergoes Hopf-bifurcation around the interior equilibrium  $E^*$ , if the following conditions are satisfied:*

- (e1)  $A_3(\eta_c)(A_1(\eta_c)A_2(\eta_c) - A_3(\eta_c)) - A_1^2(\eta_c)A_4(\eta_c) = 0$ ,
- (e2)  $\left[\text{Re}\frac{d\rho_j}{d\eta}\right]_{[\eta=\eta_c]} \neq 0$  for  $j = 1, 2$ .

**Table 3** Parameter values used for numerical simulation

Parameter	Value	Parameter	Value
$\alpha_0$	0.01	$k$	0.4
$\lambda$	0.05	$\nu$	0.01
$C_0$	280	$q_1$	500
$\theta$	0.00001	$r$	0.02
$s$	0.02	$L$	800
$\phi$	0.0002	$\pi$	0.001
$u$	0.5	$\mu$	0.1
$M$	2000	$q_2$	500
$\lambda_1$	0.00005	$\eta$	0.0002
$K$	1000		

**Remark 3** The physical interpretation of the above theorem is that as the value of  $\eta$  crosses its critical value  $\eta_c$ , the real part of at least one pair of complex eigenvalues of the Jacobian matrix at  $E^*$  changes its sign, i.e., the sign of real part of pair of complex eigenvalues changes from negative to positive or from positive to negative; therefore, the stability of the equilibrium  $E^*$  around  $\eta = \eta_c$  changes from stability to instability or instability to stability, respectively. Therefore, the Hopf-bifurcation phenomenon takes place around the interior equilibrium  $E^*$  as  $\eta$  crosses its threshold value.

### 4.1 Direction and stability of Hopf-bifurcation

In this subsection, we present the result regarding the direction and stability of bifurcating periodic solutions. The following theorem provides the information about the direction and stability of periodic solutions.

**Theorem 3** *The Hopf-bifurcation is forward (backward) if  $\mu_2 > 0$  ( $\mu_2 < 0$ ) and the bifurcating periodic solution exist for  $\eta > \eta_c$  ( $\eta < \eta_c$ ). The periodic solutions are stable or unstable according as  $\beta_2 < 0$  or  $\beta_2 > 0$  and period increases or decreases according as  $\tau_2 > 0$  or  $\tau_2 < 0$ .*

Proof of this theorem is given in Appendix C.

## 5 Numerical simulation

In this part, we present the numerical simulation to verify our analytical findings. For a hypothetical set of parameter values given in Table 3, numerical simulation has been performed using MATLAB R2013.

For the parameter values given in Table 3, conditions for existence of the interior equilibrium are satisfied. The obtained interior equilibrium  $E^*$  is given as

$$C^* = 389.7255, N^* = 769.4751, F^* = 1670.6770, B^* = 2097.2559.$$

Eigenvalues of the Jacobian matrix corresponding to  $E^*$  are given as

$$-0.0649 + 0.0188i, -0.0649 - 0.0188i, -0.0235, -0.4189.$$



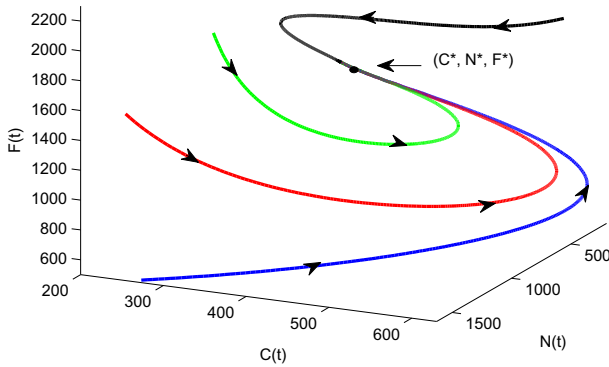


**Fig. 2** Global stability of  $(C^*, N^*, F^*)$  in  $C - N - F$  space for parameter values given in Table 3, and the initial conditions are chosen as  $(250, 1600, 1600, 1000)$ ,  $(269, 1600, 500, 1000)$ ,  $(300, 1200, 2000, 1000)$  and  $(620, 490, 2000, 1000)$

As all the eigenvalues of  $J_{E^*}$  are either negative or have negative real part which confirms that  $E^*$  is locally asymptotically stable for the chosen set of parameter values. In Fig. 2, the solution trajectories for different initial starts have been plotted for the parameter values given in Table 3. From this figure, we can see that all the solution trajectories have proceeded toward  $(C^*, N^*, F^*)$  in  $C - N - F$  space, which depicts the global stability of the interior equilibrium in  $C - N - F$  space.

Next, we have plotted the variation plots to observe the effect of some important parameters on the dynamics of considered dynamical variables. Figure 3a shows that increase in anthropogenic emission rate of  $\text{CO}_2$  ( $\lambda$ ) elevates the atmospheric level of  $\text{CO}_2$ , and because of the adverse effects of increasing  $\text{CO}_2$  on human population, population decreases; forestry biomass increases, whereas allocated budget to maintain the atmospheric level of  $\text{CO}_2$  increases. From Fig. 3b, we notice that increase in the parameter value of deforestation rate ( $\phi$ ) leads to increase in the atmospheric level of carbon dioxide which leads to increase in allocated budget for maintaining the atmospheric level of carbon dioxide. From these variation plots, we can observe that the anthropogenic emission rate of carbon dioxide and deforestation rate (i.e.,  $\lambda, \phi$ ) play an important role in the dynamics of atmospheric carbon dioxide.

Furthermore, in Fig. 4, we have plotted the atmospheric concentration of carbon dioxide with respect to time for different values of  $\nu$  and  $\mu$ , keeping rest of the parameters same as in Table 3. First, we choose  $\nu = \mu = 0$ , i.e., when the government does not take any action to reduce the atmospheric level of carbon dioxide in the considered region; the atmospheric concentration of  $\text{CO}_2$  is very high. Next, we have considered  $\nu = 0.01$  and  $\mu = 0$ , i.e., in this case, budget is used only for the decarbonization technologies and there is no afforestation/reforestation coverage in the region. In this case, the equilibrium level of concentration of atmospheric carbon dioxide is less than the equilibrium level attained in the previous case. Moreover, a substantial decrease in atmospheric concentration of carbon dioxide is noted if there is continuous growth in afforestation/reforestation coverage using budget despite the fact that efficacy of budget to control the anthropogenic emission of carbon dioxide is zero. Furthermore, we have considered that the allocated budget is used for the decarbonization techniques as well as for afforestation/reforestation. Due to the combined effect of these, the equilibrium level of atmospheric carbon dioxide settles down to a much lower value. Thus, the combined effect of decarbonization techniques and afforestation/reforestation in

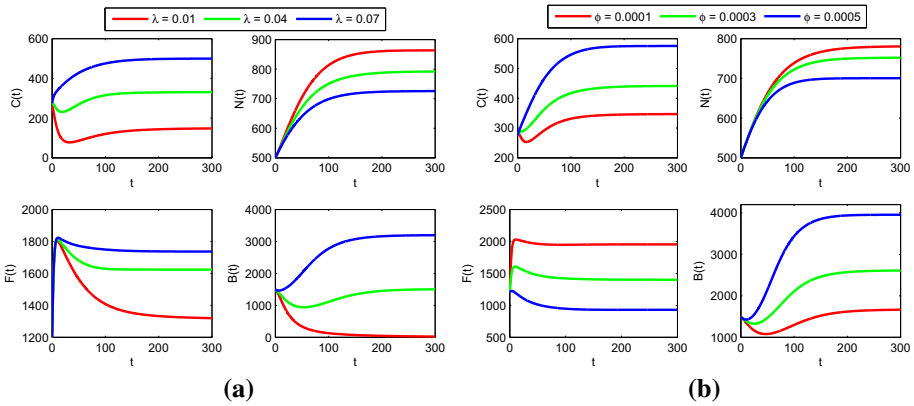


**Fig. 3** Variation of  $C(t)$ ,  $N(t)$ ,  $F(t)$ , and  $B(t)$  with respect to time  $t$  for different values of **a** anthropogenic emission rate ( $\lambda$ ) and **b** deforestation rate ( $\phi$ ). Rest of the parameters are same as in Table 3, and the initial conditions are taken as (275, 500, 1200, 1500)

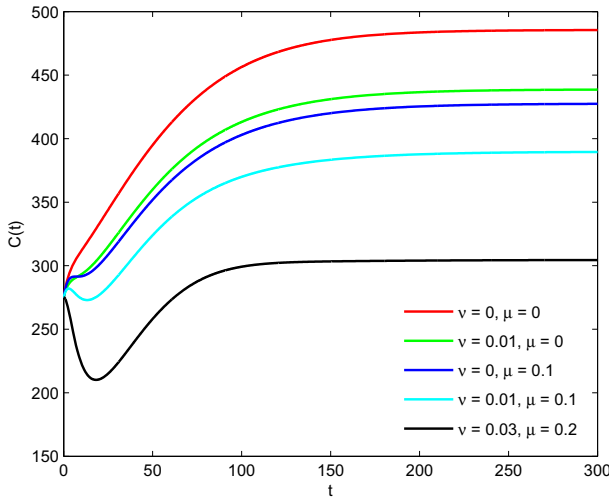


**Fig. 4** Effects of parameters  $\nu$  and  $\mu$  on atmospheric level of carbon dioxide. All the parameters are same as in Table 3, and the initial conditions are chosen as (275, 500, 1200, 1500)

the presence of budget allocation have potential to reduce the equilibrium level of atmospheric concentration of carbon dioxide.

In Fig. 5, a bar diagram has been plotted to quantify the effect of  $k$  on equilibrium level of atmospheric concentration of carbon dioxide ( $C(t)$ ) (when conditions  $\frac{dC^*}{dk} < 0$  ( $k < k_c = 0.5025$ ) and  $\frac{dC^*}{dk} > 0$  ( $k > k_c$ ) are satisfied), this figure determines the effect of fraction of budget allocation used to maintain the atmospheric level of carbon dioxide via controlling the anthropogenic emission of carbon dioxide and for afforestation/reforestation. From this figure, it can be noticed that the percentage change in equilibrium level of atmospheric carbon dioxide decreases with increase in fraction of budget used to control the anthropogenic emission of carbon dioxide up to a threshold value  $k < k_c$ . As the atmospheric level of  $CO_2$  decreases with the increase in value of  $k$  (for  $k < k_c$ ), the difference

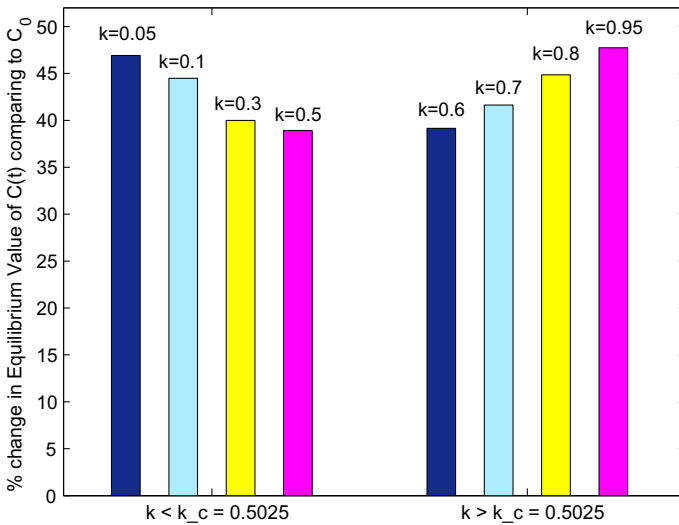


**Fig. 5** Percentage change of equilibrium level of CO<sub>2</sub> compare to pre-industrial level (C<sub>0</sub>); showing effect of increasing values of *k*. Rest of the parameters are same as given in Table 3

of atmospheric level of CO<sub>2</sub> from its pre-industrial level (C<sub>0</sub> = 280) decreases, so the percentage change decreases. In this case, fraction of budget allocation used to control the anthropogenic emission of carbon dioxide is responsible to reduce the equilibrium level of atmospheric carbon dioxide. Moreover, further increase in value *k* above a threshold value (*k* > *k<sub>c</sub>*), fraction of budget allocation used for afforestation/reforestation (i.e., 1 - *k*) is responsible to reduce the equilibrium level of atmospheric concentration of carbon dioxide. For the parameter values given in Table 3, it is observed that up to 50.25% of budget used for the control of anthropogenic emission of carbon dioxide and remaining 49.75% of budget used for afforestation/reforestation is beneficial to reduce the atmospheric level of carbon dioxide.

### 5.1 Existence of Hopf-bifurcation

To examine the existence of Hopf-bifurcation with respect to parameter *η*, we have chosen the following set of parameter values:

$$\begin{aligned}
 \alpha &= 0.01, \lambda = 0.05, \nu = 0.05, k = 0.5, q_1 = 500, \lambda_1 = 0.00005, s = 0.02, \\
 L &= 800, \theta = 0.001, \pi = 0.001, \phi = 0.0005, u = 0.5, M = 2000, \\
 \mu &= 0.01, q_2 = 500, r = 0.002, C_0 = 280, K = 1000.
 \end{aligned}
 \tag{38}$$

It is noticed that the system (1) changes its dynamics near the interior equilibrium *E\** as the growth rate of budget allocation due to increase in atmospheric level of carbon dioxide (*η*) increases. For small values of *η*, the equilibrium *E\** is stable, while the increase in value of *η* destabilizes the interior equilibrium *E\**. Further increase in value of *η* again stabilizes the interior equilibrium which clearly indicates that Hopf-bifurcation occurs twice as the value of *η* increases. Numerically, we have obtained the critical values of *η* at which change in stability occurs and they are *η<sub>1c</sub>* = 0.0007889 and *η<sub>2c</sub>* = 0.004684. We have noted that for *η* ∈ (0, *η<sub>1c</sub>*), all the eigenvalues of the Jacobian matrix at *E\** are either negative or have

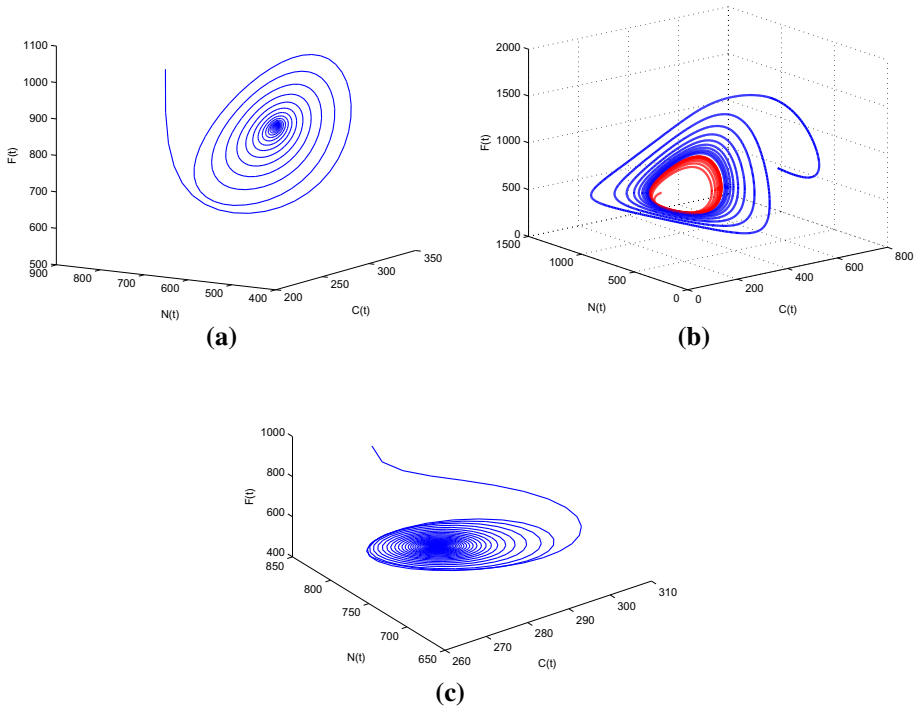


**Fig. 6** Phase portraits for system (1) in  $C - N - F$  space for different values of  $\eta$ . System shows a stability of equilibrium  $E^*$  for  $\eta = 0.0004$ , **b** appearance of limit cycle for  $\eta = 0.001$  which shows the instability of equilibrium  $E^*$ , **(c)** stability of equilibrium  $E^*$  for  $\eta = 0.008$ . Rest of the parameters are same as in (38). Initial conditions are taken as (a) (270, 800, 1500, 1000), (b) (235 800 600 3000) and (700 800 600 3000), (c) (270, 800, 1500, 1000)

negative real part showing the system (1) is stable for small values of ( $\eta < \eta_{1c}$ ); while loss of stability occurs for  $\eta = 0.0007889$  and the system remains unstable for  $\eta \in (\eta_{1c}, \eta_{2c})$ . Now, with further increase in the value of  $\eta > \eta_{2c}$ , all the eigenvalues of the Jacobian matrix corresponding to interior equilibrium  $E^*$  are negative or have negative real part, i.e., the system stabilizes for  $\eta > \eta_{2c}$ . In Fig. 6a, we draw the phase portrait in  $C - N - F$  space for  $\eta (= 0.0004) < \eta_{1c}$ , which shows that the solution trajectories are starting from outside approach toward  $E^*$ , which demonstrate that the interior equilibrium  $E^*$  is stable. In Fig. 6b for  $\eta = 0.001$ , it is shown that the solution trajectories in  $C - N - F$  space, one initiating from outside and other initiating from inside approach toward the limit cycle, which shows that the bifurcating periodic solutions are critically stable. Moreover, we have drawn the phase portrait in  $C - N - F$  space for  $\eta = 0.008 > \eta_{2c}$  in Fig. 6c, which shows that the solution trajectories are initiating from outside approach toward  $E^*$ , i.e.,  $E^*$  is stable for  $\eta > \eta_{2c}$ . To get a clear picture of the stability switch around interior equilibrium  $E^*$ , in Fig. 7, the Hopf-bifurcation diagram has been plotted considering  $\eta$  as bifurcation parameter. From this figure, we can say that on increasing the value of  $\eta$ , a stability switch for the interior equilibrium of the formulated model system occurs.

Furthermore, in Fig. 8, we have plotted the stability region with respect to parameter  $k$  and  $\eta$ , to demonstrate the relationship between these two parameters. From this figure, one can note that for small values of  $k (< 0.3693)$ , the system is stable for all values of  $\eta$  and

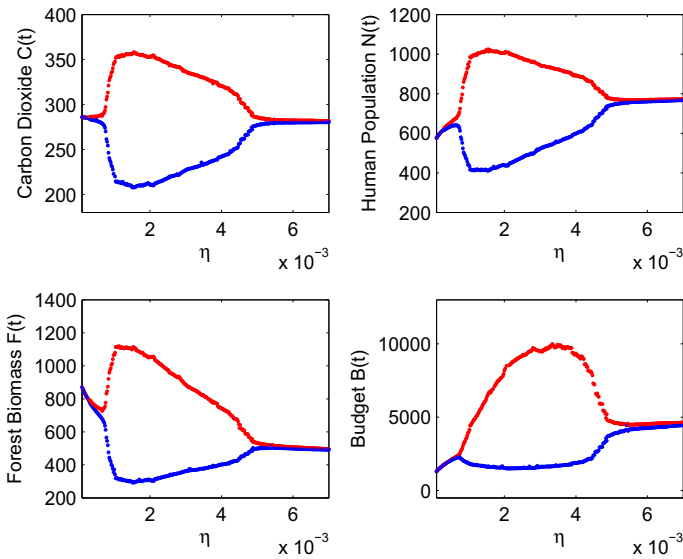


**Fig. 7** Hopf-bifurcation diagram with respect to parameter  $\eta$ . Rest of the parameters are same as in (38) and initial conditions are taken as (283, 580, 870, 2000)

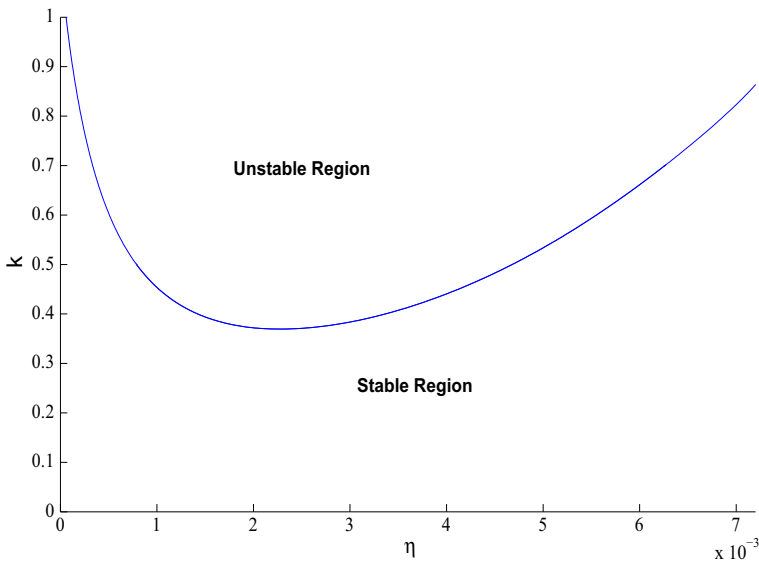


**Fig. 8** Stability region of interior equilibrium  $E^*$  for the model system (1), in  $\eta - k$  plane for the parameters given in (38)

whenever  $k > 0.3693$  a stability switch occurs for the interior equilibrium  $E^*$  with respect to bifurcating parameter  $\eta$ . Moreover, we can see that the region of instability of the interior equilibrium  $E^*$  of model system (1) with respect to bifurcating parameter  $\eta$  increases as the value of  $k$  increases.

## 6 Conclusion

Based on the present scenario of atmospheric level of carbon dioxide, it is desirable to take some initiatives for its mitigation. The prime reason for such a high level of atmospheric carbon dioxide is its anthropogenic emission, so it is required to reduce the anthropogenic emission of  $\text{CO}_2$ . For this, we have to make some mitigation strategies. As the application of any mitigation effort requires budget, therefore we have proposed a non-linear mathematical model to analyze the effect of budget on the abatement of atmospheric concentration of  $\text{CO}_2$ . For model formulation, dynamical variables as atmospheric concentration of  $\text{CO}_2$ , human population, forest biomass, and budget are considered. We have considered that the concentration of  $\text{CO}_2$  in the atmosphere increases due to its anthropogenic emissions and it depletes either naturally or its intake by the forest biomass. Human population and forestry biomass grow logistically. Human population declines due to the harmful impacts of  $\text{CO}_2$ , whereas the forest biomass declines due to deforestation by the population for their livelihood. The allocated budget is used for the control of anthropogenic emission of  $\text{CO}_2$  and reforestation/afforestation. The equilibria for the proposed model are obtained and their stability analysis has been performed. We have shown that the increment in anthropogenic emission of  $\text{CO}_2$  escalates the atmospheric level of carbon dioxide, whereas the increased rate of deforestation by the human population is also an important cause for the increased level of carbon dioxide in the atmosphere. Moreover, the strategy of using the budget for the control of anthropogenic emission of the carbon dioxide as well as for reforestation/afforestation activities would be very helpful in reducing the atmospheric level of  $\text{CO}_2$  at the desired level.

From model analysis, it has been shown that for the considered set of parameter values up to 50.25% of budget for the control of anthropogenic emission of carbon dioxide and remaining 49.75% of the budget for afforestation/reforestation is beneficial to reduce the atmospheric level of carbon dioxide. Furthermore, simulation result has indicated that if the decarbonization techniques of controlling the anthropogenic emission of carbon dioxide is not effective, then afforestation/reforestation is effective in maintaining the level of  $\text{CO}_2$  in the atmosphere. Similarly, if the afforestation/reforestation is not much effective, then one should focus on the decarbonization techniques. Furthermore, the combined effects of decarbonization techniques and afforestation/reforestation are more beneficial in maintaining the atmospheric level of carbon dioxide.

From the analysis, it is concluded that increment rate of budget for the control of increased level of carbon dioxide gives rise to interesting dynamics about the interior equilibrium  $E^*$ . It is noted that for small values of growth rate of budget allocation due to increased level of atmospheric  $\text{CO}_2$  (i.e.,  $\eta$ ), the coexisting equilibrium is stable and the increase in value of  $\eta$  destabilizes the system. However, further increase in value of  $\eta$  stabilizes the system. This shows that the coexisting equilibrium changes its stability from stable to unstable to stable as the allocated budget in proportion of increased level of atmospheric carbon dioxide increases. In terms of ecology, this situation states that for small values of increment rate of budget in proportion to increased level of carbon dioxide reduces the level of carbon dioxide in the atmosphere which leads to decrease in the allocated budget; this results to increased level of atmospheric concentration of carbon dioxide. This rise in the atmospheric level of carbon dioxide leads to increase in the allocated budget. This interplay between the atmospheric concentration of carbon dioxide and increment rate of allocated budget ( $\eta$ ) gives rise to oscillatory solution. Furthermore, increasing the value of  $\eta$  after a threshold value ( $\eta_{2c}$ ), the concentration of carbon dioxide in the atmosphere attains its saturated level and thus system gets stabilize. Furthermore, increase in value of  $\eta$  does not affect the stability of system

and the system remains stable for all increase in  $\eta > \eta_{2c}$ . Model analysis reveals that the anthropogenic emission of carbon dioxide and deforestation due to human population has much impact on the atmospheric level of carbon dioxide, but the level of CO<sub>2</sub> can be reduced to a desired level by making proper strategy using budget allocation. Also, the funding for research and development of new technologies is an important aspect for moving forward in the field of maintaining the atmospheric level of carbon dioxide.

**Acknowledgements** The corresponding author is thankful to Innovation in Science Pursuit for Inspired Research (INSPIRE), Department of Science and Technology, Government of India for providing financial support in the form of junior research fellowship (No: DST/INSPIRE Fellowship/2018/IF180791).

## Appendix A

**Proof** From the third equation of the model system (1), we have

$$\frac{dF}{dt} \leq uF \left( 1 - \frac{F}{M} \right) + \mu F.$$

Using the theory of differential inequality, we have

$$\limsup_{t \rightarrow \infty} F(t) \leq \frac{M(u + \mu)}{u} = F_m \text{ (say).}$$

From the second equation of model system, we have

$$\frac{dN}{dt} \leq (s + \pi \phi F_m)N - \frac{sN^2}{L}.$$

Using the same argument as before

$$\limsup_{t \rightarrow \infty} N(t) \leq \frac{L}{s}(s + \pi \phi F_m) = N_m \text{ (say).}$$

Now, from the first equation of the model system

$$\frac{dC}{dt} \leq -\alpha(C - C_0) + \lambda N_m.$$

Then, we have

$$\limsup_{t \rightarrow \infty} C(t) \leq \frac{\alpha C_0 + \lambda N_m}{\alpha}.$$

Similarly, we can show that

$$\limsup_{t \rightarrow \infty} B(t) \leq \frac{K}{r} \left( r + \frac{\eta \lambda N_m}{\alpha} \right).$$

□

## Appendix B

**Proof** For any  $N \geq 0$ , we have  $\left. \frac{dN}{dt} \right|_{N=0} = 0$  which implies that  $N = 0$  is invariant manifold. Due to continuity of system, we can conclude that  $N$  would never go below zero if its initial

condition is non-negative. Therefore

$$\begin{aligned} \frac{dC}{dt} &\geq \alpha C_0 - \alpha C - \frac{vkB_m}{q_1 + kB_m} N_m - \lambda_1 C F_m. \\ \Rightarrow \liminf_{t \rightarrow \infty} C(t) &\geq \frac{\left(\alpha C_0 - \frac{vkB_m}{q_1 + kB_m} N_m\right)}{\alpha + \lambda_1 F_m} = C_a \text{ (say),} \end{aligned}$$

provided that  $\left(\alpha C_0 - \frac{vkB_m}{q_1 + kB_m} N_m\right) > 0$ . Moreover

$$\begin{aligned} \frac{dB}{dt} &\geq rB - \frac{rB^2}{K} + \eta(C_a - C_0)B, \\ \Rightarrow \liminf_{t \rightarrow \infty} B(t) &\geq \frac{K}{r} \{r + \eta(C_a - C_0)\} = B_a \text{ (say),} \end{aligned}$$

provided  $r + \eta(C_a - C_0) > 0$ . From third equation of the model system (1), we have

$$\begin{aligned} \frac{dF}{dt} &\geq uF - \frac{uF^2}{M} - \phi N_m F + \frac{\mu(1-k)B_a}{q_2 + (1-k)B_a} F, \\ \Rightarrow \liminf_{t \rightarrow \infty} F(t) &\geq \frac{M}{u} \left(u - \phi N_m + \frac{\mu(1-k)B_a}{q_2 + (1-k)B_a}\right) = F_a \text{ (say),} \end{aligned}$$

provided that  $\left(u - \phi N_m + \frac{\mu(1-k)B_a}{q_2 + (1-k)B_a}\right) > 0$ . From the second equation of the model (1), we have

$$\begin{aligned} \frac{dN}{dt} &\geq sN - \frac{sN^2}{L} - \theta(C_m - C_0)N + \pi\phi F_a N, \\ \Rightarrow \liminf_{t \rightarrow \infty} N(t) &\geq \frac{L}{s} (s - \theta(C_m - C_0) + \pi\phi F_a) = N_a \text{ (say),} \end{aligned}$$

provided that  $(s - \theta(C_m - C_0) + \pi\phi F_a) > 0$ . Taking  $M_1 = \min(C_a, N_a, F_a, B_a)$ , we have

$$M_1 \leq \liminf_{t \rightarrow \infty} (C(t), N(t), F(t), B(t)),$$

, and from Lemma 1, the system is uniformly bounded. Hence, the system is persistence.  $\square$

### Appendix C

**Proof** In this part, we will proof the result for direction of bifurcating periodic solutions. For this, we translate the origin to the interior equilibrium  $E^*$ , by substituting  $C = C^* + x_1$ ,  $N = N^* + x_2$ ,  $F = F^* + x_3$  and  $B = B^* + x_4$ , where  $x = (x_1, x_2, x_3, x_4)^T$  are small perturbation. Now, we have following system:

$$\begin{pmatrix} \frac{dx_1}{dt} \\ \frac{dx_2}{dt} \\ \frac{dx_3}{dt} \\ \frac{dx_4}{dt} \end{pmatrix} = \begin{pmatrix} g_1(x_1, x_2, x_3, x_4) \\ g_2(x_1, x_2, x_3, x_4) \\ g_3(x_1, x_2, x_3, x_4) \\ g_4(x_1, x_2, x_3, x_4) \end{pmatrix} + O(|x|^3),$$



where

$$\begin{aligned}
 g_1(x_1, x_2, x_3, x_4) &= -(\alpha + \lambda_1 F^*)x_1 + \left(\lambda - \frac{vkB^*}{q_1 + kB^*}\right)x_2 - \lambda_1 C^*x_3 - \frac{q_1 k v N^*}{(q_1 + kB^*)^2}x_4 \\
 &\quad - \lambda_1 x_1 x_3 - \frac{vkq_1 x_2 x_4}{(q_1 + kB^*)^2} + \frac{vq_1 k^2 N^* x_4^2}{(q_1 + kB^*)^3}, \\
 g_2(x_1, x_2, x_3, x_4) &= -\theta N^*x_1 - \frac{sN^*}{L}x_2 + \pi\phi N^*x_3 - \frac{sx_2^2}{L} - \theta x_1 x_2 + \pi\phi x_2 x_3, \\
 g_3(x_1, x_2, x_3, x_4) &= -\phi F^*x_2 - \frac{uF^*}{M}x_3 + \frac{q_2\mu(1-k)F^*}{(q_2 + (1-k)B^*)^2}x_4 - \frac{ux_3^2}{M} - \phi x_2 x_3 \\
 &\quad + \frac{\mu q_2(1-k)x_3 x_4}{(q_2 + (1-k)B^*)^2} - \frac{\mu(1-k)^2 q_2 F^* x_4^2}{(q_2 + (1-k)B^*)^3}, \\
 g_4(x_1, x_2, x_3, x_4) &= \eta B^*x_1 - \frac{rB^*}{K}x_4 - \frac{rx_4^2}{K} + \eta x_1 x_4.
 \end{aligned}$$

In the above expression, we are not interested in coefficient of third or higher degree. Now, the system takes the form

$$\dot{x} = J^*x + G(x), \tag{.1}$$

where

$$x = \begin{pmatrix} x_1 \\ x_2 \\ x_3 \\ x_4 \end{pmatrix}, J^* = \begin{pmatrix} -(\alpha + \lambda_1 F^*) \left(\lambda - \frac{vkB^*}{q_1 + kB^*}\right) - \lambda_1 C^* & \frac{-q_1 k v N^*}{(q_1 + kB^*)^2} \\ -\theta N^* & 0 \\ 0 & -\phi F^* \\ \eta B^* & 0 \end{pmatrix} \begin{pmatrix} \frac{-q_1 k v N^*}{(q_1 + kB^*)^2} \\ 0 \\ \frac{q_2\mu(1-k)F^*}{(q_2 + (1-k)B^*)^2} \\ -\frac{rB^*}{K} \end{pmatrix}$$

and

$$G(x) = \begin{pmatrix} g_1 \\ g_2 \\ g_3 \\ g_4 \end{pmatrix} = \begin{pmatrix} -\lambda_1 x_1 x_3 - \frac{vkq_1 x_2 x_4}{(q_1 + kB^*)^2} - \frac{vq_1 k^2 N^* x_4^2}{(q_1 + kB^*)^3} \\ -\frac{sx_2^2}{L} - \theta x_1 x_2 + \pi\phi x_2 x_3 \\ -\frac{ux_3^2}{M} - \phi x_2 x_3 + \frac{\mu q_2(1-k)x_3 x_4}{(q_2 + (1-k)B^*)^2} + \frac{\mu(1-k)^2 q_2 F^* x_4^2}{(q_2 + (1-k)B^*)^3} \\ -\frac{rx_4^2}{K} + \eta x_1 x_4 \end{pmatrix}.$$

The eigenvectors  $u_1, u_2,$  and  $u_3$  of the Jacobian matrix  $J^*$  corresponding to the eigenvalues  $i\omega_0, \rho_3,$  and  $\rho_4$  are obtained as follows:

$$\begin{aligned}
 u_1 &= \begin{pmatrix} u_{11} - iu_{12} \\ u_{21} - iu_{22} \\ u_{31} - iu_{32} \\ u_{41} - iu_{42} \end{pmatrix}, u_2 = \begin{pmatrix} u_{13} \\ u_{23} \\ u_{33} \\ u_{43} \end{pmatrix}, \\
 u_3 &= \begin{pmatrix} u_{14} \\ u_{24} \\ u_{34} \\ u_{44} \end{pmatrix}.
 \end{aligned}$$

Here

$$\begin{aligned}
 u_{11} &= -\frac{rB^*}{K} \left( \frac{sN^*}{L} \frac{uF^*}{M} - \omega^2 + \pi\phi^2 N^* F^* \right) + \omega^2 \left( \frac{sN^*}{L} + \frac{uF^*}{M} \right), \\
 u_{12} &= -\left\{ \frac{rB^*}{K} \omega \left( \frac{sN^*}{L} + \frac{uF^*}{M} \right) - \omega \left( \frac{sN^*}{L} \frac{uF^*}{M} - \omega^2 + \pi\phi^2 N^* F^* \right) \right\}, \\
 u_{21} &= \frac{\theta N^*}{\eta B^*} \left( \frac{rB^*}{K} \frac{uF^*}{M} - \omega^2 \right) - \frac{\pi\phi N^* q_2 \mu (1-k) F^*}{(q_2 + (1-k)F^*)^2}, \\
 u_{22} &= \left\{ \frac{\omega\theta N^*}{\eta B^*} \left( \frac{rB^*}{K} + \frac{uF^*}{M} \right) \right\}, \\
 u_{31} &= -\frac{sN^*}{L} \frac{q_2 \mu (1-k) F^*}{(q_2 + (1-k)B^*)^2} - \phi F^* \frac{\theta N^*}{\eta B^*} \frac{rB^*}{K}, \\
 u_{32} &= -\left\{ \frac{\omega q_2 \mu (1-k) F^*}{(q_2 + (1-k)B^*)^2} + \frac{\omega\phi F^* \theta N^*}{\eta B^*} \right\}, \\
 u_{41} &= -\frac{sN^*}{L} \frac{uF^*}{M} + \omega^2 - \pi\phi^2 N^* F^*, \\
 u_{42} &= -\omega \left( \frac{sN^*}{L} + \frac{uF^*}{M} \right), \\
 u_{13} &= -\left( \frac{rB^*}{K} + \lambda_3 \right) \left[ \left( \frac{sN^*}{L} + \lambda_3 \right) \left( \frac{uF^*}{M} + \lambda_3 \right) + \pi\phi^2 N^* F^* \right], \\
 u_{23} &= \frac{\theta N^*}{\eta B^*} \left( \frac{rB^*}{K} + \lambda_3 \right) \left( \frac{uF^*}{M} + \lambda_3 \right) - \frac{\pi\phi N^* q_2 \mu (1-k) F^*}{(q_2 + (1-k)B^*)^2}, \\
 u_{33} &= -\left( \frac{sN^*}{L} + \lambda_3 \right) \left( \frac{q_2 \mu (1-k) F^*}{q_2 + (1-k)B^*)^2} - \frac{\phi F^* \theta N^*}{\eta B^*} \left( \frac{rB^*}{K} + \lambda_3 \right) \right), \\
 u_{43} &= -\left( \frac{sN^*}{L} + \lambda_3 \right) \left( \frac{uF^*}{M} + \lambda_3 \right) - \pi\phi^2 N^* F^*, \\
 u_{14} &= -\left( \frac{rB^*}{K} + \lambda_4 \right) \left[ \left( \frac{sN^*}{L} + \lambda_4 \right) \left( \frac{uF^*}{M} + \lambda_4 \right) + \pi\phi^2 N^* F^* \right], \\
 u_{24} &= \frac{\theta N^*}{\eta B^*} \left( \frac{rB^*}{K} + \lambda_3 \right) \left( \frac{uF^*}{M} + \lambda_3 \right) - \frac{\pi\phi N^* q_2 \mu (1-k) F^*}{(q_2 + (1-k)B^*)^2}, \\
 u_{34} &= -\left( \frac{sN^*}{L} + \lambda_4 \right) \left( \frac{q_2 \mu (1-k) F^*}{q_2 + (1-k)B^*)^2} - \frac{\phi F^* \theta N^*}{\eta B^*} \left( \frac{rB^*}{K} + \lambda_4 \right) \right), \\
 u_{44} &= -\left( \frac{sN^*}{L} + \lambda_4 \right) \left( \frac{uF^*}{M} + \lambda_4 \right) - \pi\phi^2 N^* F^*.
 \end{aligned}$$

Define  $U = (Re(u_1), -Im(u_1), u_2, u_3)$ , that is

$$U = \begin{pmatrix} u_{11} & u_{12} & u_{13} & u_{14} \\ u_{21} & u_{22} & u_{23} & u_{24} \\ u_{31} & u_{32} & u_{33} & u_{34} \\ u_{41} & u_{42} & u_{43} & u_{44} \end{pmatrix}.$$

The matrix  $U$  is non-singular, such that

$$U^{-1}PU = \begin{pmatrix} 0 & -\omega_0 & 0 & 0 \\ \omega_0 & 0 & 0 & 0 \\ 0 & 0 & \rho_3 & 0 \\ 0 & 0 & 0 & \rho_4 \end{pmatrix}.$$

Inverse of matrix  $U$  is given by

$$U^{-1} = \begin{pmatrix} y_{11} & y_{12} & y_{13} & y_{14} \\ y_{21} & y_{22} & y_{23} & y_{24} \\ y_{31} & y_{32} & y_{33} & y_{34} \\ y_{41} & y_{42} & y_{43} & y_{44} \end{pmatrix}.$$

$$y_{11} = \frac{1}{\Delta} [u_{22}(u_{33}u_{44} - u_{34}u_{43}) + u_{23}(u_{42}u_{34} - u_{44}u_{32}) + u_{24}(u_{43}u_{32} - u_{42}u_{33})],$$

$$y_{12} = \frac{1}{\Delta} [u_{12}(u_{43}u_{34} - u_{44}u_{33}) + u_{13}(u_{32}u_{44} - u_{34}u_{42}) + u_{14}(u_{33}u_{42} - u_{43}u_{32})],$$

$$y_{13} = \frac{1}{\Delta} [u_{12}(u_{44}u_{23} - u_{43}u_{24}) + u_{13}(u_{42}u_{24} - u_{44}u_{22}) + u_{14}(u_{43}u_{22} - u_{23}u_{42})],$$

$$y_{14} = \frac{1}{\Delta} [u_{12}(u_{24}u_{33} - u_{23}u_{34}) + u_{13}(u_{22}u_{34} - u_{32}u_{24}) + u_{14}(u_{23}u_{32} - u_{33}u_{22})],$$

$$y_{21} = \frac{1}{\Delta} [u_{21}(u_{34}u_{43} - u_{44}u_{33}) + u_{23}(u_{44}u_{31} - u_{34}u_{41}) + u_{24}(u_{41}u_{33} - u_{31}u_{43})],$$

$$y_{22} = \frac{1}{\Delta} [u_{11}(u_{33}u_{44} - u_{34}u_{43}) + u_{13}(u_{34}u_{41} - u_{44}u_{31}) + u_{14}(u_{31}u_{43} - u_{33}u_{41})],$$

$$y_{23} = \frac{1}{\Delta} [u_{11}(u_{43}u_{24} - u_{44}u_{23}) + u_{13}(u_{21}u_{44} - u_{24}u_{41}) + u_{14}(u_{41}u_{23} - u_{43}u_{21})],$$

$$y_{24} = \frac{1}{\Delta} [u_{11}(u_{23}u_{34} - u_{24}u_{33}) + u_{13}(u_{31}u_{24} - u_{34}u_{21}) + u_{14}(u_{33}u_{21} - u_{23}u_{31})],$$

$$y_{31} = \frac{1}{\Delta} [u_{21}(u_{32}u_{44} - u_{42}u_{34}) + u_{22}(u_{34}u_{41} - u_{31}u_{44}) + u_{24}(u_{31}u_{42} - u_{32}u_{41})],$$

$$y_{32} = \frac{1}{\Delta} [u_{11}(u_{42}u_{34} - u_{44}u_{32}) + u_{12}(u_{44}u_{31} - u_{34}u_{41}) + u_{14}(u_{41}u_{32} - u_{42}u_{31})],$$

$$y_{33} = \frac{1}{\Delta} [u_{11}(u_{44}u_{22} - u_{42}u_{24}) + u_{12}(u_{41}u_{24} - u_{21}u_{44}) + u_{14}(u_{41}u_{32} - u_{42}u_{31})],$$

$$y_{34} = \frac{1}{\Delta} [u_{11}(u_{32}u_{24} - u_{34}u_{22}) + u_{12}(u_{21}u_{34} - u_{24}u_{31}) + u_{14}(u_{22}u_{31} - u_{21}u_{32})],$$

$$y_{41} = \frac{1}{\Delta} [u_{21}(u_{42}u_{33} - u_{43}u_{32}) + u_{22}(u_{43}u_{31} - u_{33}u_{41}) + u_{23}(u_{41}u_{32} - u_{31}u_{42})],$$

$$y_{42} = \frac{1}{\Delta} [u_{11}(u_{43}u_{32} - u_{42}u_{33}) + u_{12}(u_{33}u_{41} - u_{31}u_{43}) + u_{13}(u_{42}u_{31} - u_{32}u_{41})],$$

$$y_{43} = \frac{1}{\Delta} [u_{11}(u_{42}u_{23} - u_{43}u_{22}) + u_{12}(u_{43}u_{21} - u_{23}u_{41}) + u_{13}(u_{41}u_{22} - u_{21}u_{42})],$$

$$y_{44} = \frac{1}{\Delta} [u_{11}(u_{33}u_{22} - u_{32}u_{23}) + y_{12}(u_{31}u_{23} - u_{21}u_{33}) + u_{13}(u_{32}u_{21} - u_{31}u_{22})].$$

Consider the transformation  $x = Uw$ , i.e.,  $w = U^{-1}x$ , where  $w = (w_1, w_2, w_3, w_4)$ . Under the linear transformation, the system takes the form

$$\dot{w} = (U^{-1}J^*U)w + g(w), \tag{.2}$$

where  $g(w) = U^{-1}G(Uw)$ . This can be written as

$$\begin{aligned} \dot{w}_1 &= -\omega_0 w_2 + g^1(w_1, w_2, w_3, w_4) \\ \dot{w}_2 &= -\omega_0 w_1 + g^2(w_1, w_2, w_3, w_4) \\ \dot{w}_3 &= \rho_3 w_3 + g^3(w_1, w_2, w_3, w_4) \\ \dot{w}_4 &= \rho_4 w_4 + g^4(w_1, w_2, w_3, w_4), \end{aligned}$$

where  $g = (g^1, g^2, g^3, g^4)^T$

$$\begin{aligned} g^1 &= y_{11}h_1 + y_{12}h_2 + y_{13}h_3 + y_{14}h_4, \\ g^2 &= y_{21}h_1 + y_{22}h_2 + y_{23}h_3 + y_{24}h_4, \\ g^3 &= y_{31}h_1 + y_{32}h_2 + y_{33}h_3 + y_{34}h_4, \\ g^4 &= y_{41}h_1 + y_{42}h_2 + y_{43}h_3 + y_{44}h_4; \end{aligned}$$

here,

$$\begin{aligned} h_1 &= -\lambda_1(u_{11}w_1 + u_{12}w_2 + u_{13}w_3 + u_{14}w_4)(u_{31}w_1 + u_{32}w_2 + u_{33}w_3 + u_{34}w_4) \\ &\quad - \frac{vkq_1(u_{21}w_1 + u_{22}w_2 + u_{23}w_3 + u_{24}w_4)(u_{41}w_1 + u_{42}w_2 + u_{43}w_3 + u_{44}w_4)}{(q_1 + kB^*)^2} \\ &\quad - \frac{vq_1^2k^2N^*}{(q_1 + kB^*)^2}(u_{41}w_1 + u_{42}w_2 + u_{43}w_3 + u_{44}w_4)^2, \\ h_2 &= -\frac{s}{L}(u_{21}w_1 + u_{22}w_2 + u_{23}w_3 + u_{24}w_4)^2 - \theta(u_{11}w_1 + u_{12}w_2 + u_{13}w_3 + u_{14}w_4) \\ &\quad (u_{21}w_1 + u_{22}w_2 + u_{23}w_3 + u_{24}w_4) \\ &\quad + \pi\phi(u_{21}w_1 + u_{22}w_2 + u_{23}w_3 + u_{24}w_4)(u_{31}w_1 + u_{32}w_2 + u_{33}w_3 + u_{34}w_4), \\ h_3 &= -\frac{u}{M}(u_{31}w_1 + u_{32}w_2 + u_{33}w_3 + u_{34}w_4)^2 - \phi(u_{21}w_1 + u_{22}w_2 + u_{23}w_3 + u_{24}w_4) \\ &\quad (u_{31}w_1 + u_{32}w_2 + u_{33}w_3 + u_{34}w_4) \\ &\quad + \frac{\mu(1-k)^2q_2^2F^*}{(q_2 + (1-k)B^*)^3}(u_{41}w_1 + u_{42}w_2 + u_{43}w_3 + u_{44}w_4)^2 \\ &\quad + \frac{\mu q_2(1-k)}{(q_2 + (1-k)B^*)^2}(u_{31}w_1 + u_{32}w_2 + u_{33}w_3 + u_{34}w_4) \\ &\quad \times (u_{41}w_1 + u_{42}w_2 + u_{43}w_3 + u_{44}w_4), \\ h_4 &= -\frac{r}{K}(u_{41}w_1 + u_{42}w_2 + u_{43}w_3 + u_{44}w_4)^2 + \eta(u_{11}w_1 + u_{12}w_2 + u_{13}w_3 + u_{14}w_4) \\ &\quad (u_{41}w_1 + u_{42}w_2 + u_{43}w_3 + u_{44}w_4). \end{aligned}$$

Furthermore, we can calculate  $h_{11}, h_{02}, h_{20}, H_{21}, H_{110}^1, H_{110}^2, H_{101}^1, H_{101}^2, \sigma_{11}^1, \sigma_{11}^2, \sigma_{20}^1, \sigma_{20}^2$  following the procedure given in Hassard et al (Hassard *et al.* 1981). Using the above, we

can find the following quantities:

$$\begin{aligned}
 h_{21} &= H_{21} + 2(H_{110}^1 \sigma_{11}^1 + H_{110}^2 \sigma_{11}^2) + H_{101}^1 \sigma_{20}^1 + H_{101}^2 \sigma_{20}^2, \\
 c_1(0) &= \frac{i}{2\omega_0} \left( h_{11} h_{20} - 2|h_{11}|^2 - \frac{|h_{02}|^2}{3} \right) + \frac{h_{21}}{2}, \\
 \mu_2 &= -\frac{\operatorname{Re}(c_1(0))}{\phi'(0)}, \\
 \tau_2 &= -\frac{(\operatorname{Im}(c_1(0)) + \mu_2 \sigma'(0))}{\omega_0}, \\
 \beta_2 &= -2\mu_2 \phi'(0),
 \end{aligned}$$

where,  $\phi'(0) = \frac{d}{d\eta} (\operatorname{Re}(\rho(\eta)))|_{\eta=\eta_c}$  and  $\sigma'(0) = \frac{d}{d\eta} (\operatorname{Im}(\rho(\eta)))|_{\eta=\eta_c}$ .  $\square$

## References

- Atmospheric level of carbon dioxide (2021): <https://www.esrl.noaa.gov/gmd/ccgg/trends/global.html> Accessed 12 Feb 2021
- Caetano MAL, Gherardi DFM, Yoneyama T (2011) An optimized policy for the reduction of  $C O_2$  emission in the Brazilian Legal Amazon. *Ecol Modell* 222(15):2835–2840. <https://doi.org/10.1016/j.ecolmodel.2011.05.003>
- Casper JK (2010) Greenhouse gases: worldwide impacts, Infobase Publishing
- Cropper M, Griffiths C (1994) The interaction of population Growth and environmental quality. *Am Econ Rev* 84(2): 250–254 <https://www.jstor.org/stable/2117838>
- Devi S, Gupta N (2020) Comparative study of the effects of different growths of vegetation biomass on  $C O_2$  in crisp and fuzzy environments. *Nat Resour Model* 33(2):e12263. <https://doi.org/10.1111/nrm.12263>
- FAO and UNEP (2020) The state of the world's forests 2020. Forests, Biodiversity and People, Rome. <https://doi.org/10.4060/ca8642en>. Accessed 20 April 2021
- Fawzy S, Osman AI, Doran J, Rooney DW (2020) Strategies for mitigations of climate change: a review. *Environ Chem Lett* 18:2069–2094. <https://doi.org/10.1007/s10311-020-01059-w>
- Fuss S, Lamb WF, Callaghan MW, Hilaire J, Creutzig F, Amann T, Beringer T, W de Oliveira Garcia, Hartmann J, Khanna T, Luderer G (2018) Negative emissions -Part 2: Costs, potentials and side effects. *Environ Res Lett* 13(6) <https://doi.org/10.1088/1748-9326/aabf9f>
- Gasser T, Guivarch C, Tachiiri K, Jones CD, Ciais P (2015) Negative emissions physically needed to keep global warming below 2°C. *Nat Commun* 6. <https://doi.org/10.1038/ncomms8958>
- Gibbins J, Chalmers H (2008) Carbon capture and storage. *Energy policy* 36(12):4317–22. <https://doi.org/10.1016/j.enpol.2008.09.058>
- Hassard BD, Kazarinoff ND, Wan YH (1981) Theory and Applications of Hopf-bifurcation. Cambridge University Press, Cambridge
- IPCC (2014) Climate Change 2014: Mitigation of Climate Change. Contribution of working group III to the fifth assessment report of intergovernmental panel on climate change [Edenhofer, O., Piche-Madruga, R., Sokona, Y., Farahani, E., Kadner, S., Seyboth, K., Adler, A., Baum, I., Brunner's, Eickemeyer, P., Remann, B., Savolainen, J., Schlomer, S., Von Stechow, C., Zwickel, T., and Minx, J.C. (eds.)]. Cambridge University Press, Cambridge, United Kingdom and New York, NY, USA. [https://www.ipcc.ch/site/assets/uploads/2018/03/WGIIIAR5\\_SPM\\_TS\\_Volume-3.pdf](https://www.ipcc.ch/site/assets/uploads/2018/03/WGIIIAR5_SPM_TS_Volume-3.pdf) Accessed 20 April 2021
- IPCC (2018) Global Warming of 1.5°C. In: Masson-Delomette V, Zhai P, Portner HO, Roberta D, Skea J, Shukla PR, Pirani A, Moufouma-Okia W, Pean C, Pidcock R, Connors S, Matthews JBR, Chen Y, Zhou X, Gomis MI, Lonny E, Maycock T, Tignor M, Waterfield T (eds.) An IPCC Special Report on the impacts of global warming of 1.5°C above pre-industrial levels and related global greenhouse gas emission pathways, in the context of strengthening the global response to the threat of climate change, sustainable development, and efforts to eradicate poverty. [https://www.ipcc.ch/sites/assets/uploads/sites/2/2019/06/SR15\\_Full\\_Report\\_High\\_Res.pdf](https://www.ipcc.ch/sites/assets/uploads/sites/2/2019/06/SR15_Full_Report_High_Res.pdf) Accessed 20 April 2021
- Lata K, Misra AK (2017) Modeling the effect of economic efforts to control population pressure and conserve forestry resources. *Nonlinear Anal: Model Cont* 22(4): 473–488 <https://doi.org/10.15388/NA.2017.4.4>
- Misra AK, Jha A (2021) Modeling the effect of population pressure on the dynamics of carbon dioxide gas. *J Appl Math Comput* 67:623–640. <https://doi.org/10.1007/s12190-020-01492-8>

- Misra AK, Verma M (2013) A mathematical model to study the dynamics of carbon dioxide gas in the atmosphere. *Appl Math Comput* 219(16):8595–8609. <https://doi.org/10.1016/j.amc.2013.02.058>
- Misra AK, Verma M (2015) Impact of environmental education on mitigation of carbon dioxide emissions: a modelling study. *Int J Glob Warm* 7(4):466–486
- Misra AK, Lata K, Shukla JB (2014) Effects of population and population pressure on forest resources and their conservation: a modeling study. *Environ Dev Sustain* 16:361–374. <https://doi.org/10.1007/s10668-013-9481-x>
- MoEFCC (2021) India: Third biennial update report to the united nations framework Convention on Climate Change. Ministry of Environment, Forest and Climate Change, Government of India. [https://unfccc.int/sites/default/files/resource/INDIA%20BUR-3\\_20.02.2021\\_High.pdf](https://unfccc.int/sites/default/files/resource/INDIA%20BUR-3_20.02.2021_High.pdf) Accessed 25 April 2021
- Nikol'skii MS (2010) A controlled model of carbon circulation between the atmosphere and the ocean. *Comput Math Model* 21:414–424. <https://doi.org/10.1007/s10598-010-9081-7>
- Onozaki K (2009) Population is a critical factor for global carbon dioxide increase. *J Health Sci* 55:125–127. <https://doi.org/10.1248/jhs.55.125>
- Pires JCM (2019) Negative emissions technologies: a complementary solution for climate change mitigation. *Sci Total Environ* 672:502–514. <https://doi.org/10.1016/j.scitotenv.2019.04.004>
- Ricke KL, Millar RJ, MacMartin DG (2017) Constraints on global temperature target overshoot. *Sci Rep* 7:14743. <https://doi.org/10.1038/s41598-017-14503-9>
- Shi A (2003) The impact of population pressure on global carbon dioxide emissions, 1975–1996: evidence from pooled cross-country data. *Ecol Econ* 44(1):29–42. [https://doi.org/10.1016/S0921-8009\(02\)00223-9](https://doi.org/10.1016/S0921-8009(02)00223-9)
- Shukla JB, Lata K, Misra AK (2011) Modeling the depletion of a renewable resource by population and industrialization: effect of technology on its conservation. *Nat Resour Model* 24(2):242–267. <https://doi.org/10.1111/j.1939-7445.2011.00090.x>
- Shukla JB, Chauhan MS, Sundar S, Naresh R (2015) Removal of carbon dioxide from the atmosphere to reduce global warming: a modeling study. *Int J Glob Warm* 7(2):270–292. <https://doi.org/10.1504/IJGW.2015.067754>
- Smith P, Davis SJ, Creutzig F, Fuss S, Minx J, Gabrielle B, Kato E, Jackson RB, Cowie A, Kriegler E, Van Vuuren DP (2016) Biophysical and economic limits to negative  $CO_2$  emissions. *Nat Clim Change* 6(1):42–50. <https://doi.org/10.1038/nclimate2870>
- Tennakone K (1990) Stability of the biomass-carbon dioxide equilibrium in the atmosphere: mathematical model. *Appl Math Comput* 35:125–130. [https://doi.org/10.1016/0096-3003\(90\)90113-H](https://doi.org/10.1016/0096-3003(90)90113-H)
- UNCCS (2019) Climate action and support trend, United Nations Climate Change Secretariat. [https://unfccc.int/sites/default/files/resource/Climate\\_Action\\_Support\\_Trends\\_2019.pdf](https://unfccc.int/sites/default/files/resource/Climate_Action_Support_Trends_2019.pdf) Accessed 20 April 2021
- United Nations Environment Programme 2019. Emission Gap Report 2019. UNEP, Nairobi. <http://www.unenvironment.org/emissionsgap> Accessed 25 Apr 2021
- Verma M, Misra AK (2018) Optimal control of anthropogenic carbon dioxide emissions through technological options: a modelling study. *Comput Appl Math* 37(1):605–626. <https://doi.org/10.1007/s40314-016-0364-2>
- Vinca A, Rottoli M, Marangoni G, Tavoni M (2018) The role of carbon capture and storage electricity in attaining 1.5 and 2°C. *Int J Greenh Gas Control* 78:148–159. <https://doi.org/10.1016/j.ijggc.2018.07.020>
- Wee JH (2013) A review on carbon dioxide capture and storage technology using coal fly ash. *Appl Energy* 106:143–151. <https://doi.org/10.1016/j.apenergy.2013.01.062>

**Publisher's Note** Springer Nature remains neutral with regard to jurisdictional claims in published maps and institutional affiliations.